

56795

LACUSTRINE MINERAL FACIES OF THE NEOGENE  
PELİTÇİK BASIN (GALATEAN VOLCANIC PROVINCE)

A THESIS SUBMITTED TO  
THE GRADUATE SCHOOL OF NATURAL AND APPLIED SCIENCES OF  
THE MIDDLE EAST TECHNICAL UNIVERSITY

BY

MEHMET LÜTFİ SÜZEN

56795

IN PARTIAL FULFILLMENT OF THE REQUIREMENTS  
FOR THE DEGREE  
OF

MASTER OF SCIENCE

IN

THE DEPARTMENT OF GEOLOGICAL ENGINEERING

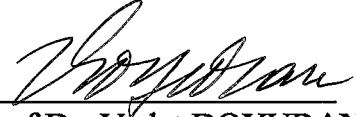
JUNE 1996

Approval of the Graduate School of Natural and Applied Sciences



Prof. Dr. Tayfur Öztürk  
Director

I certify that this thesis satisfies all the requirements as a thesis for the degree of Master of Science



Prof. Dr. Vedat DOYURAN  
Head of Department

This is to certify that we have read this thesis and that our opinion it is fully adequate, in scope and quality, as a thesis for the degree of Master of Science



Assoc. Prof. Dr. Asuman TÜRK MENOĞLU  
Supervisor

Examining Committee Members

Prof. Dr. Vedat DOYURAN



Assoc. Prof. Dr. Asuman TÜRK MENOĞLU



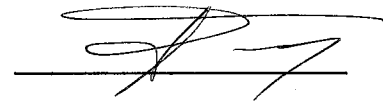
Assoc. Prof. Dr. Vedat TOPRAK



Assoc. Prof. Dr. Ayla TANKUT



Assoc. Prof. Dr. Emel BAYHAN



## **ABSTRACT**

### **LACUSTRINE MINERAL FACIES OF THE NEOGENE PELİTÇİK BASIN (GALATEAN VOLCANIC PROVINCE)**

Süzen, Mehmet Lütfi

M.S. Department of Geological Engineering

Supervisor: Assoc.Prof.Dr. Asuman TÜRKMENOĞLU

June 1996, 106 pages

The geology and mineralogy of the Neogene lacustrine facies (Pazar formation) of Pelitçik basin were investigated by means of remote sensing, field and laboratory studies. The data obtained from remote sensing, field, petrography, X-ray diffraction, scanning electron microscope and Fourier Transform infrared radiation studies were used to determine the paleoenvironmental parameters of this Neogene lacustrine basin.

The laboratory studies indicate that dolomite and K-feldspar are the major non-clay minerals in the study area, where, plagioclase, analcime,

erionite (?) and quartz are the minor constituents. Dolomites are found to be non-stoichiometric in chemistry by means of X-ray diffraction studies. The clay fraction of Pazar formation is dominantly composed of dioctahedral smectites. The smectites are rich in Al-Fe, which indicates a detrital origin. Illite has a minor contribution to the clay fraction, where, chlorite and kaolinite are found in trace amounts.

Based on dolomite stoichiometry and mineral paragenesis found in Pelitçik basin, the depositional conditions of the lake is inferred as, perennial, shallow and quiet lacustrine environment with fresh to slightly saline and slightly alkaline water chemistry. In addition, the lake has started its evolution with a hydrologically open system model and completed its evolution with a hydrologically closed system.

**Key words:** Pelitçik Basin, Galatean Volcanic Province, Lacustrine Mineral Facies, Clay Mineralogy, Dolomite Stoichiometry, Paleoenvironment, Remote Sensing.

## ÖZ

### NEOJEN YAŞLI PELİTÇİK HAVZASINDAKİ GÖLSEL MİNERAL FASİYESLERİ (GALATYA VOLKANİK PROVENSİ)

Süzen, Mehmet Lütfi

Yüksek Lisans, Jeoloji Mühendisliği Bölümü

Tez Yöneticisi: Doç.Dr. Asuman TÜRKMENOĞLU

Haziran 1996, 106 sayfa

Pelitçik Havzasında yüzeyleyen Neojen gölssel fasiyeslerin (Pazar formasyonu) jeolojisi ve mineralojisi uzaktan algılama, arazi ve laboratuvar çalışmaları ile araştırılmıştır. Uzaktan algılama, arazi, petrografi, X-ışınları difraksiyonu, tarama elektron mikroskopu ve Fourier Dönüşümü kızıl ötesi ışınım yöntemleri ile elde edilen veriler Pelitçik gölssel havzanın paleo-ortamsal özelliklerini ortaya çıkartmakta kullanılmıştır.

Laboratuvar çalışmaları, çalışma alanında dolomit ve K-feldispat grubu minerallerin ağırlıklı olarak kil dışı mineralleri oluşturduğunu göstermiştir.

Bunun yanı sıra plajioloklas, analsim, eriyonit (?) ve kuvars da az miktarda saptanmıştır. X-ışınları difraksiyon çalışmaları dolomitlerin kimyasal olarak stokyometrik olmadığını ortaya koymuştur. Pazar formasyonunun kil fraksiyonu ise çoklukla dioktahedral smektitlerden oluşmaktadır. Fe-Al ce zengin olan smektitler detritik kökene sahiptirler. İllit, klorit ve kaolin minerallerine ise eser miktarlarda rastlanmıştır.

Dolomit stokyokimyasına ve mineral parajenezine dayanarak, Pelitçik havzası depolanma koşullarının; mevsim değişikliklerinde kurumayan, sığ, sakin gölssel bir ortam; su kimyası için ise tatlı sudan, az tuzlu suya değişen ve az alkalin bir ortam olduğu bulunmuştur. Ayrıca, havzanın evrimine, hidrolojik olarak, açık bir sistemde başladığı ve evrimini kapalı bir sistemde sonucuna varılmıştır.

**Anahtar Kelimeler:** Pelitçik Havzası, Galatya Volkanik Provensi, Gölssel Mineral Fasiyesleri, Kil Mineralojisi, Dolomit Stokyokimyası, Paleo-ortam, Uzaktan Algılama.

## ACKNOWLEDGMENTS

I express my special thanks to my supervisor Assoc.Prof.Dr. Asuman TÜRKMENOĞLU, for her continued support, guidance, encouragement and enthusiasm throughout the whole study.

My special thanks goes to the General Directorate of the Mineral Research and Exploration (MTA) and to the Chemical Engineering Department (METU) for providing laboratory facilities during X-ray diffraction studies. Special thanks are due to Prof.Dr. Ali ÇULFAZ, Dr.AKIN GEVEN, Miss. Serap İÇÖZ, Mr. T.Ahmet URAL and Mr. Halil KALIPÇILAR who very kindly took time out of their overloaded schedule and gave valuable help, constructive comments, and suggestions.

I would like to thank to Assoc.Prof.Dr.Vedat TOPRAK for his enormous support and guidance in field and remote sensing studies.

I am also grateful to Dr.Cengiz TAN for SEM, to Hasan BÖKE for FTIR, to Orhan KARAMAN and Ahmet UYANKAYA for their supports.

I would also like to thank to Mr.Arda ARCASOY, Mr.Erhan KANSU and to my friends for their continuous encouragement throughout the study.

I, finally, should express my ultimate gratitude for my family and for Miss.Ufuk GÜVEN in favor of their support and thrust in each single minute of this study.

## TABLE OF CONTENTS

ABSTRACT . . . . .	iii
ÖZ . . . . .	v
ACKNOWLEDGMENT . . . . .	vii
LIST OF TABLES . . . . .	xi
LIST OF FIGURES . . . . .	xii
CHAPTERS	
1.INTRODUCTION . . . . .	1
1.1. PURPOSE AND SCOPE . . . . .	1
1.2. GEOGRAPHIC SETTING . . . . .	2
1.3. PREVIOUS WORKS . . . . .	4
1.3.1. Previous works on the regional geology . . . . .	4
1.3.2. Previous works on lake clays and associated minerals in volcanic regions . . . . .	10
1.4. REGIONAL GEOLOGY . . . . .	12
1.5. METHODS OF INVESTIGATION . . . . .	14
1.5.1. Remote Sensing studies . . . . .	14
1.5.2. Digital Elevation Model (DEM) studies . . . . .	15
1.5.3. Field studies . . . . .	16
1.5.4. Laboratory studies . . . . .	16



2. GEOLOGY . . . . .	19
2.1. GENERAL GEOLOGY . . . . .	19
2.2. STRATIGRAPHY . . . . .	28
2.2.1. Neogene Volcanics . . . . .	28
2.2.1.1. General Definition . . . . .	28
2.2.1.2. Distribution and boundaries . . . . .	28
2.2.1.3. Lithology . . . . .	29
2.2.1.4. Age . . . . .	32
2.2.2. Pazar formation . . . . .	32
2.2.2.1. General Definition . . . . .	32
2.2.2.2. Distribution, Boundaries and Thickness . . . . .	33
2.2.2.3. Lithology . . . . .	33
2.2.2.4. Age . . . . .	39
2.2.3. Quaternary Alluvium . . . . .	41
3. MINERALOGY . . . . .	42
3.1. THIN SECTION STUDIES . . . . .	42
3.1.1. Yoncatepe Section . . . . .	43
3.1.2. Buğralar Section . . . . .	46
3.1.3. Akkayatepe section . . . . .	49
3.2. X-RAY DIFFRACTION STUDIES . . . . .	53
3.2.1. Non-clay Mineralogy . . . . .	53
3.2.2. Dolomite Stoichiometry . . . . .	59

3.2.3. Clay Mineralogy . . . . .	63
3.3. FOURIER TRANSFORM INFRARED RADIATION STUDIES . . . . .	67
3.4. SCANNING ELECTRON MICROSCOPE STUDIES . . . . .	71
4. DISCUSSION OF RESULTS . . . . .	82
4.1. GEOLOGY . . . . .	82
4.2. MINERALOGY . . . . .	85
5. CONCLUSIONS . . . . .	91
REFERENCES . . . . .	94
APPENDICES	
A PREPARATION OF CLAY SAMPLES FOR X-RAY DIFFRACTION ANALYSES . . . . .	102
B PREPARATION OF PELLETS FOR INFRARED ANALYSES . . . . .	104
C <i>d</i> SPACING VALUES OF STUDIED K-FELDSPARS, PLAGICLASES AND DOLOMITES in PAZAR FORMATION . . . . .	105

## LIST OF TABLES

3.1. X-ray Diffraction data of investigated dolomites . . . . .	61
3.2. Fourier Transform Infrared Radiation absorbtions of samples of Pazar formation . . . . .	70



## LIST OF FIGURES

1.1.	Location map of the study area . . . . .	3
1.2.	Regional geologic setting of the study area . . . . .	13
2.1.	Geologic map of the study area . . . . .	20
2.2.	Landsat 5 TM image of the study area . . . . .	21
2.3.	3-dimensional view of the study area based on Landsat False Color (Red=7, Green=5, Blue=3) composite . . . . .	22
2.4.	Relief image of the study area and its vicinity . . . . .	23
2.5.	Digital Elevation Model of the study area and its vicinity . . . . .	24
2.6.	Field view of the Bayındır fault scarp . . . . .	26
2.7.	Generalized stratigraphic section of the Pelitçik Basin . . . . .	27
2.8.	Field view of Sarıkavak Tuff . . . . .	30
2.9.	Field view of volcanoclastic deposits . . . . .	30
2.10.	Cross bedding in the upper parts of volcanoclastic deposits . . . . .	31
2.11.	Measured Stratigraphic Section of Yoncatepe Sequence . . . . .	34
2.12.	Location of Yoncatepe Measured Stratigraphic Section . . . . .	35
2.13.	Measured Stratigraphic Section of Buğralar Sequence . . . . .	37
2.14.	Field view of Buğralar Measured Stratigraphic sequence . . . . .	38
2.15.	Volcanoclastic lens at the base of Buğralar sequence . . . . .	38

2.16.	Measured Stratigraphic Section of Akkayatepe Sequence . . .	40
2.17.	Field view of Akkayatepe measure stratigraphic sequence . . .	41
3.1.	Photomicrograph showing Multiple Rim Accretionary Lapilli . . . . .	44
3.2.	Photomicrograph showing feldspars (f) and volcanic rock fragments in crystal vitric tuff . . . . .	44
3.3.	Photomicrograph showing pumice fragments (p) in vitric tuff . . . . .	45
3.4.	Photomicrograph showing glass shards (g) vitric tuff . . . . .	45
3.5.	Photomicrograph showing siliceous shell bearing organisms (Diatomacea ?) in claystone, (d) Diatomacea . . . . .	47
3.6.	Photomicrograph showing dolomicrite rhombs in argillaceous dolomicrites, (d) dolomite . . . . .	47
3.7.	Photomicrograph showing dolomicrite rhombs in argillaceous dolomicrites, (d) dolomite . . . . .	48
3.8.	Photomicrograph showing the aragonite cement of cherty limestone facies, (a) Aragonite . . . . .	48
3.9.	Photomicrograph showing the microdolomite rhombs embedded in clayey matrix . . . . .	50
3.10.	Photomicrograph showing the gypsum vein in argillaceous dolomicrite facies, (g) gypsum . . . . .	50
3.11.	Photomicrograph showing the general view of the crystal vitric tuff . . . . .	51
3.12.	Photomicrograph showing the general view of vitric tuff (g) glass shard . . . . .	51
3.13.	Photomicrograph showing the general view of argillaceous dolomicrite facies . . . . .	52
3.14.	Photomicrograph showing the calcite (c) precipitation in the walls of solution cavities . . . . .	53

3.15. X-ray diffraction patterns of unoriented whole-rock samples of Yoncatepe sequence . . . . .	55
3.16. X-ray diffraction patterns of unoriented whole-rock samples of Buğralar sequence . . . . .	57
3.17. X-ray diffraction patterns of unoriented whole-rock samples of Akkayatepe sequence . . . . .	58
3.18. The X-ray diffraction peaks of dolomite . . . . .	60
3.19. Scattergram showing the relation of ordering ratio with %CaCO <sub>3</sub> . . . . .	62
3.20. Trends in dolomite stoichiometry data and inferred precipitational conditions . . . . .	62
3.21. X-ray diffraction patterns of clay fraction (<2μ) of Pazar formation . . . . .	65
3.22. α (060) peaks of selected smectites . . . . .	66
3.23. Fourier Transform Infrared Radiation spectras of Pazar formation . . . . .	69
3.24. Scanning electron micrograph showing lenticular structure of Diatomacea (?) . . . . .	72
3.25. Scanning electron micrograph showing the limbs and slits of Diatomacea (?) . . . . .	72
3.26. Scanning electron micrograph showing dolomite rhombs and its EDX . . . . .	73
3.27. Scanning electron micrograph showing authigenic K-feldspar crystals . . . . .	74
3.28. Scanning electron micrograph showing authigenic K-feldspars in analcime rich mudstone and its EDX . . . . .	75
3.29. Scanning electron micrograph showing analcime crystals and its EDX . . . . .	77
3.30. Scanning electron micrograph showing fibrous zeolites (Erionite ? or mordenite ?) on silicified wood . . . . .	78

3.31. Scanning electron micrograph showing internal structure of pumice particles . . . . .	78
3.32. Scanning electron micrograph showing a well preserved glass shard . . . . .	79
3.33. Scanning electron micrograph showing the close up view of relations between a pumice fragment and authigenically grown smectites . . . . .	79
3.34. Scanning electron micrograph showing a glass shard and its EDX . . . . .	80
3.35. Scanning electron micrograph showing authigenic smectites grown in the pore spaces of pumices . . . . .	81
3.36. Scanning electron micrograph showing the typical honeycomb structure of smectites . . . . .	81
C.1. d spacing and 2 theta values of K-feldspars . . . . .	105
C.2. d spacing values of dolomite . . . . .	106

# CHAPTER 1

## INTRODUCTION

### 1.1. PURPOSE AND SCOPE

Volcanic regions are one of the most economically important geologic sites in the world, beyond the scope of their valuable metalliferous deposits, geothermal resources and their embedded lacustrine sedimentary basins. Zeolites, various clay beds such as kaolins and bentonites, coal beds, saline minerals and tuffs exhibit extensive potential in the various world auctions. A brief look up to the habitudes of these minerals will greatly show their importance. Zeolites are used for filtering of drinking water and poisoned blood, tuffaceous rocks are good raw material resources for ceramic industry whereas, among the clay deposits, bentonite has vast consumption fields in drilling, winery, soap industry and used as supplementary material in various sectors of industry.

Galatean Volcanic Province being one of the greatest volcanic fields of Turkey has attracted several mining companies for its economic resources. There have been numerous attempts for gold and precious metal prospection in the last few years. Furthermore, the economic sedimentary



basins of Galatean Volcanic Province take out some of the attraction. This significant progress in this field which is one of the reasons that led the author to conduct this research in order to find the mineral associations and their source relations in the greatest Neogene lacustrine sedimentary basin (Pelitçik Basin) of Galatean Volcanic Province.

The aim of this study is to utilize Remote Sensing and field studies in order to construct a general stratigraphic section for the basin fill deposits and a geologic map of the Pelitçik basin. The relationships of mineral associations and paleo-environmental parameters are aimed to study with petrography, X-ray diffraction, scanning electron microscope and Fourier Transform Infrared Radiation methods, which constitute the major scope of this study. In addition, creating a geological and mineralogical database of this Neogene lacustrine basin will serve as a milestone for further economical studies and mineral prospections. On the other hand the structure, evolution and aerial distribution of volcanics in the study area, strictly falls out of the scope.

## **1.2. GEOGRAPHIC SETTING**

The study area is located in Central Anatolia, approximately at 75 km NW of Ankara (Figure 1.1). The geologically mapped terrain is approximately 400 square kilometers and lies in H28-b1, H28-b2, H28-b3, H29-a1 quadrangles of the 1:25.000 scaled topographic maps of Bolu. Main settlements in the study area are Peçenek, Pelitçik, Osmansın, Yoncatepe,

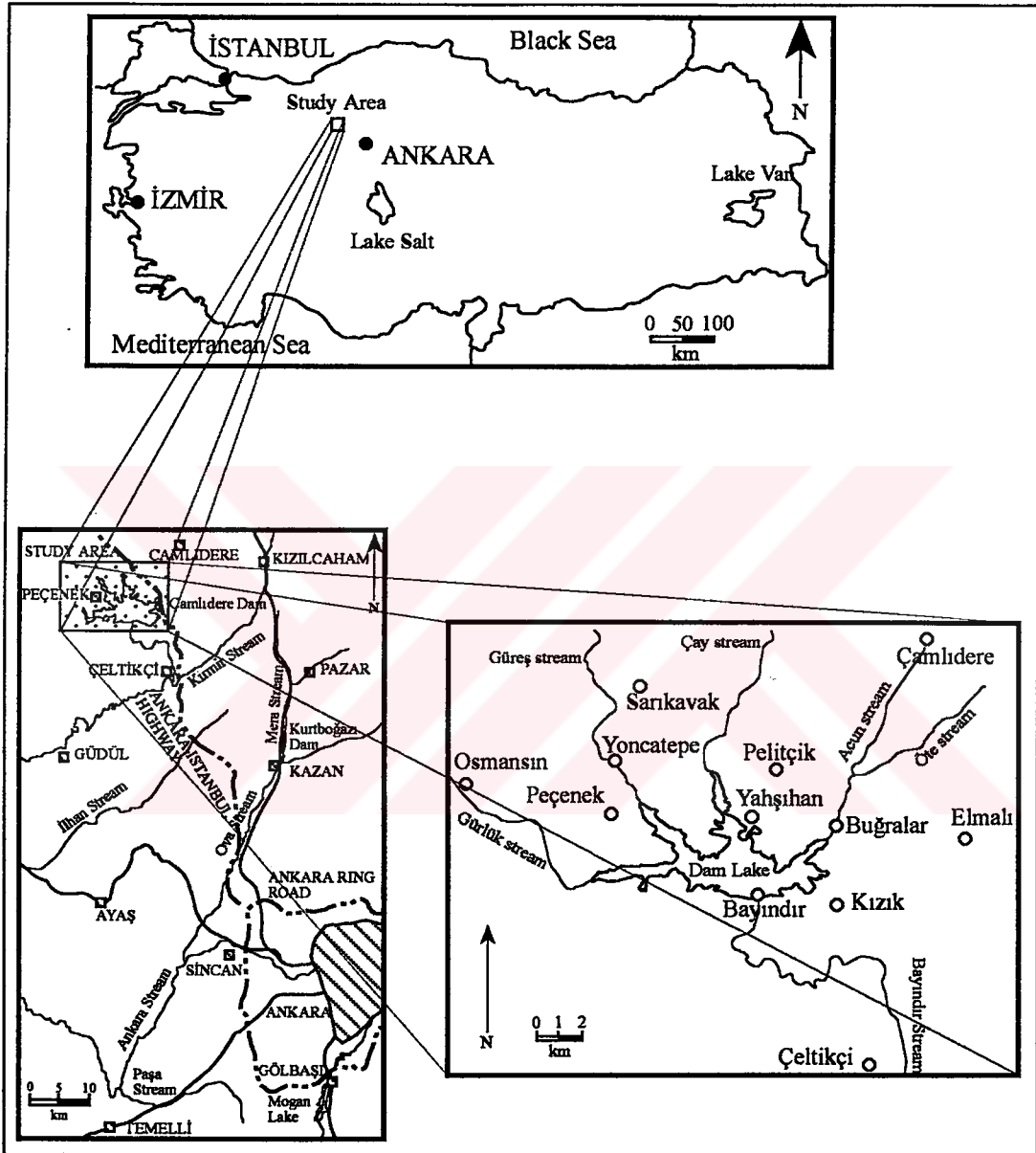


Figure 1.1: Location map of the study area

Sarıkavak, Yahşihan, Buğralar, Kızık, Bayındır and Elmalı villages. Main streams of the study area are Gürlük, Güreş, Çay, Acun, Öte and Bayındır streams. Two manmade engineering structures are also located in the study area, the Ankara-İstanbul autoroad and the Çamlıdere dam and its reservoir.

### **1.3. PREVIOUS WORKS**

Previous studies are compiled under two major headings: previous works on the regional geology and previous works on the lake clays and associated minerals in volcanic regions.

#### **1.3.1. Previous works on the regional geology:**

There are a number of studies in the literature, which deals with the geology, geochemistry, economic geology and petrogenesis of the volcanics and associated rocks in the Galatean Volcanic Province. Stchepinsky (1942), Kleinsorge (1943), Bender (1955), Erol (1955), Rondot (1956), Nebert (1959), Kalafatçioğlu and Uysallı (1964), were the first authors that named and studied the regional geology and geothermal resources of the Galatean Volcanic Province. The above authors all agree that the age of the Galatean Volcanic Province falls into Tertiary period and the main rock types are andesitic-dacitic lavas, their associated pyroclastics, basaltic lavas, Neogene continental to lacustrine facies and Quaternary alluviums. However, the age,

stratigraphic position and the internal structure of the Galaetan volcanics are inadequately mentioned.

Akyol (1969) have studied the lignite occurrences at Çeltikçi and Kızılcahamam. He stated that, after a significant volcanic eruption, at the quiet period, a marn sequence with thin coal layers had been deposited in a lake. Palynologic determinations yielded as Middle Miocene age to that lake. The similar palynologic facies of Beypazarı coals lead Akyol to a result that, Çeltikçi lignites and Beypazarı coals were formed in the same lake.

Çopur (1972) studied the general geology and investigated the clay potential of Ankara in 7 selected areas. DTA analyses and ceramic analyses were done on selected clay samples of Çamlıdere-Peçenek area. He found that the clay occurrences in this basin were of bentonitic character, and the lake sediments were rich in diatomite frustules in some outcrops. He also confirmed that Çamlıdere - Pelitçik basin had a limited but prospective clay potential.

Özkuzey and Ünsal (1972) elaborated the reserve capacity and properties of perlite occurrences around Ankara - Kızılcahamam. They mentioned about a volcanic eruption center at Yukarı and Aşağı Ovacık villages.

Ünlü (1973), studied the geology and geothermal energy potential of Kazanlar - Peçenek area, NW of Ankara. He had distinguished

stratigraphically two types of lavas, Early Miocene lower lavas and Miocene intermediate lavas, and found that the volcanism had reached to a peak period at Early Miocene times. Furthermore, he interpreted the types and morphology of the volcanics. He concluded that in Late Miocene times, a lake, having a shore at Doğanlar-Sarıkavak-Osmansın villages, spread to S-SE and the lacustrine facies are now represented by tuffite - agglomerate, tuff - marn, tuff - tuffite - limestone alternations. He also stated that the lake environment was characterized by vast amounts of plants, slightly agitated, and sometimes a bit saline character.

Tatlı (1975), studied the geology and geothermal resources of eastern Kızılcahamam geothermal field. He had differentiated the lithostratigraphic units of Kızılcahamam area. He also suggested that Pazar Formation reflects the Miocene lake, of which its basin fill deposits were not only vertically but also horizontally intercalated with volcanic rocks.

Öngür (1976, 1977) studied the Neogene stratigraphy, volcano-stratigraphy, volcanology, petrology, petrography and geothermal energy potential of the Çamlıdere, Çeltikçi and Kazan districts. He had named 5 different lavas (lower lavas, Aluç lava, Binkoz lava, Tekke lava and Karalar lava), numbers of tuff layers and three eruption centers (Aluç, Binkoz and Ağacın eruption centers). He also stated that the volcanism occurred in two phases and both phases had calcalkaline characters.

Turgut (1978) studied the lignite potential of amlıdere and eltiki areas. He pointed out that there were sixteen lignite outcrops in the area but none of them were significant. Three deep drill holes were opened but no significant lignites were cut. In this study palynologic data indicated that the age of the lignites in the basin were Middle Miocene.

Varol and Kazancı (1980) studied the volcanosediments of Galatean Volcanic Province in Seben region. They stated that the volcanics were represented by epiclastics in Upper Cretaceous, but in Miocene they were characterized by mostly as pyroclastics which filled up the Miocene lakes.

Okay and Grsoy (1984) studied the geothermal potential of Kızılcahamam-Gerede district by geophysical (gravitational) methods. They mentioned two important faults in the investigated area, the eltiki fault and a fault lying between Peenek and Sorgun villages and passing through Bayındır village. They also stated that Peenek basin was bounded by dense material (volcanic rocks) from the western side and the basinfill rocks could be traced under these volcanic rocks.

Tankut and Trkmenođlu (1988) studied the petrography and geochemistry of the Neogene mafic lavas around Ankara. They found that, the basic volcanics were in alkaline character representing a primary magma composition, of which they were derived from a mantle lherzolite source. They also suggested that magma had been modified with LIL enriched mantle in later stages of development.

Tankut *et al.* (1990) studied the geochemistry of Tertiary volcanic rocks of northwest Central Anatolia. It was stated that the volcanism had started in Eocene with calcalkaline character, and continued in Pliocene with alkaline character.

Türkmenoğlu *et al.* (1990) studied the petrography and mineralogy of the Kemeres tuff unit at Karasar district. They pointed out the depositional environment of this tuff unit as a saline-alkaline Miocene lake based on the occurrences of authigenic mineral assemblage (Montmorillonite + Phillipsite + Clinoptilolite).

Türkecan *et al.* (1991) studied the geology and petrology of the Galatean Volcanic Province. They have extensively mapped and differentiated the lithologies of the western part of the Galatean Volcanic Province. They concluded that the Neogene volcanism started at least at Early Miocene times, with radioisotopic age dating and paleontological observations. They had also studied the petrochemistry of the volcanic rocks. They stated that Late Cretaceous and Paleocene volcanics were arc volcanics, Miocene volcanics were Andean type continental margin volcanics, and Early Pliocene volcanics were alkaline with shoshonitic properties.

Keller *et al.* (1992) studied the chemical characters and ages of Galatean Volcanic Province. The chemical data derived from this study

outlines three major magmatic series: rhyolites, calc-alkaline andesite-dacites and alkaline basalts. The Neogene andesitic volcanics had an age span of 20-18 Ma., however the Neogene basaltic volcanics had an age of 11.6 to 9.6 Ma.

Tankut *et al.* (1995) studied the petrogenesis of Galatean Volcanic Province. They found two different volcanic periods in the Galatean Volcanic Province based on K/Ar ratio, first in Early Miocene and the second in Late Miocene. Early Miocene volcanics were represented by rocks of basalt-andesite-dacite-rhyolite lavas and associated pyroclastics which had been erupted from strato-volcanoes. However, the Late Miocene volcanics were composed of only basaltic rocks. The young series were related with post-tectonic extensional events, and the older ones were related with syn- or post-collisional lithospheric extension. They had also pointed out and dated five volcanic subcomplexes of the Galatean Volcanic Province, as Koroğlu-Kartalkaya, Kavaklıdağ, Orta, Daskamun and Ovacık volcanic complexes. All of these complexes are dated as Early Miocene by radioisotopic dating. However they mentioned about two other complexes around Kızılcahamam and its vicinity, but they could not give the exact locations of these volcanic eruption centers.



### **1.3.2. Previous works on lake clays and associated minerals in volcanic regions:**

Studies dealt with the lake clays and associated minerals in volcanic regions comprise a huge body of work, hence the most critical key references will be pointed out here in this section.

The water chemistry of lakes in volcanic regions do range from highly alkaline-highly saline compositions to slightly alkaline-dilute compositions. This broad range of water chemistry is directly affected from the geochemistry of surrounding rocks and the degree of evaporation in the lake basin. Moreover the water chemistry itself directly affects the type of the mineral that has to be formed authigenically (Surdam and Parker, 1972; Boles and Surdam, 1979; Hay and Guldman, 1987; Remy and Ferrell, 1989; Sheppard 1989; Sheppard, 1991; Sheppard, 1994 and Stamatakis, 1989b).

The vast diversity of authigenic silicate minerals have been reported by various authors in the literature. However, among these diverse associations, the dominance of smectite and zeolite group minerals should have to be noticed. Suitable water chemistry and readily deposited unstable glassy (vitric) tuffs or volcanics presumably governs the authigenic growth of smectites, often prior to zeolite group minerals in volcanic lakes (Surdam and Parker, 1972; Khury and Eberl, 1979; Sheppard, 1989; Stamatakis, 1989 a, b; Altaner and Grim, 1990; de Pablo-Galan, 1990; Banfield *et al.*, 1991; Sheppard, 1994).

Immoderately saline lakes in volcanic regions basically induce the authigenic growth of various types of zeolites. Clinoptilolite, analcime, chabazite, phillipsite, mordenite and erionite are the usual authigenic zeolites that form in volcanic lakes. These silicates chiefly correspond to alkaline conditions and result from the reaction of unstable volcanic glass, mostly tuff, with interstitial waters (Hay, 1966, 1978; Surdam, 1977; Surdam and Sheppard, 1978 and Chamley, 1989).

Following the progressive path of diagenesis, zeolite group minerals and then, using the early formed zeolites as precursors, K-feldspars occur with or without the smectite phase. Furthermore the lateral and vertical zonation of these authigenic silicates should have to be mentioned, unless the basin is disturbed by later tectonic forces (Sheppard and Gude, 1968; Mariner and Surdam, 1970; Surdam and Parker, 1972; Surdam and Sheppard, 1978; Hay, 1978; Boles and Surdam, 1979; Jones and Weir, 1983; Hay and Guldman, 1987; Remy and Ferrell, 1989; Sheppard and Fitzpatrick, 1989; Sheppard, 1989; Stamatakis, 1989 a, b; Altaner and Grim, 1990; de Pablo-Galan, 1990; Banfield *et al.*, 1991 and Sheppard, 1991, 1994).

Despite the authigenic mineral assemblages of lakes in volcanic regions there is also a detrital supply to these lakes. The major constituents of this detrital supply are dioctahedral smectites, K-feldspars, illites, chlorites, volcanic glass, various types of silica, plagioclases, pyroxenes,

amphiboles, smectite mixed layers and kaolinite (Swain, 1966; Nelson, 1967; Grim, 1968; Degens *et al.*, 1971). Beyond the scope of detrital clay minerals in volcanic environments, smectite group chiefly attracts the most attention. In areas where acidic volcanic products are abundant it is inevitable to record the presence of illite and smectite as weathering products (Grim, 1968). However the outstanding features of these smectites are their dioctahedral structure and their Fe-Al or Mg bearing behaviors (Jones and Weir, 1983; Chamley, 1989).

#### 1.4. REGIONAL GEOLOGY

The regional geologic setting of the study area can be best evaluated when it is described in relation to the regional geology of Galatean Volcanic Province.

Galatean Volcanic Province, which is located at northwest of Ankara (Figure 1.2), lies within the Pontide tectonic unit (Ketin, 1966). It is one of the largest Cenozoic volcanic areas of Turkey, which is composed of numbers of eruption centers and Neogene continental basins (Ünlü, 1973; Tatlı, 1975; Öngür, 1977; Türkecan *et al.*, 1991 and Tankut *et al.*, 1995). The regional tectonic character had been gained by northward subduction of İzmir-Ankara-Erzincan ocean (Northern branch of NeoTethys) and the collision of African Plate and Eurasian Plate during Alpine Orogenesis in general sense (Şengör and Yılmaz, 1981; Koçyiğit, 1991). This collision is yielded as the andesitic-dacitic volcanic associations of the Galatean

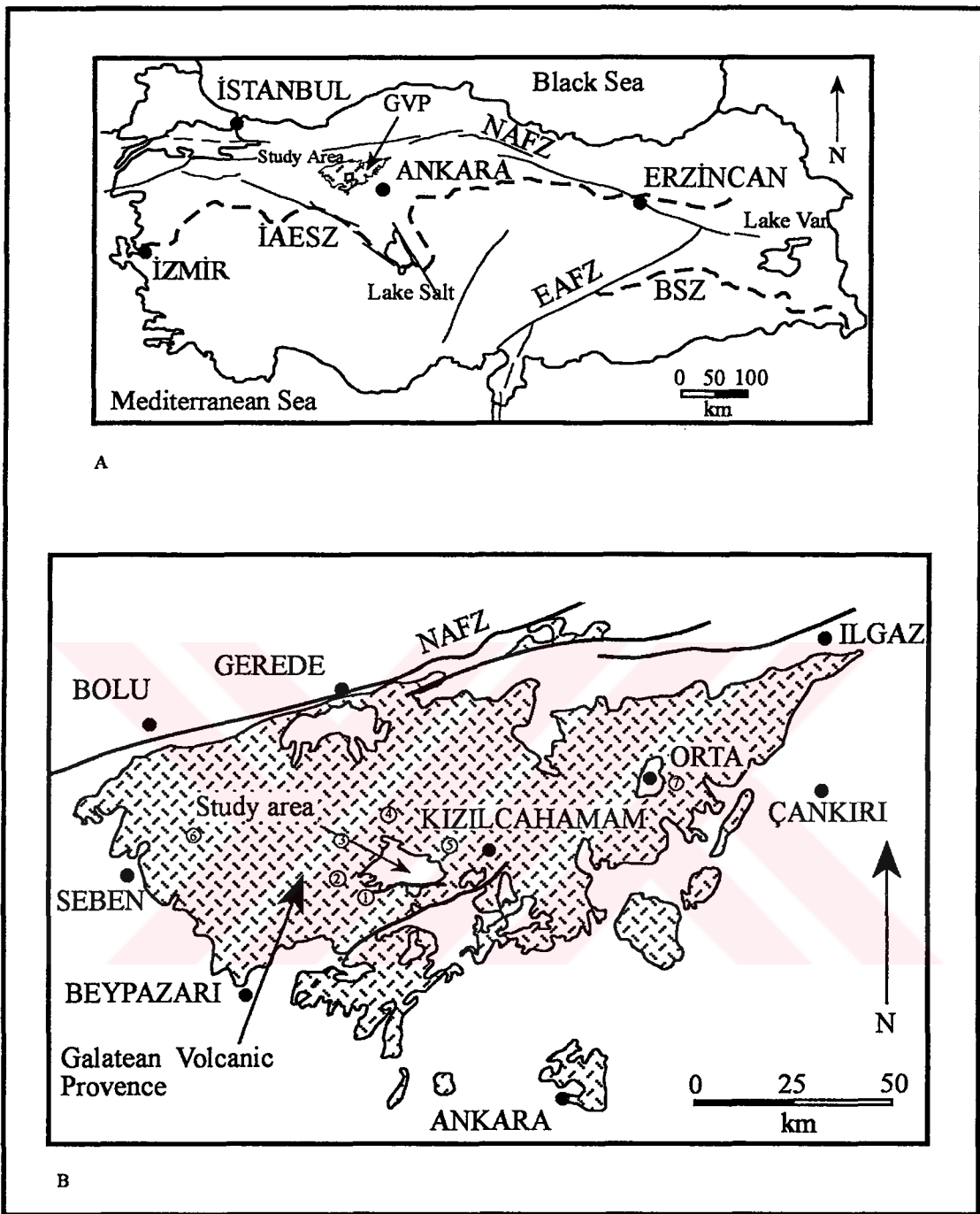


**Figure 1.2.:** Regional geologic setting of the study area. A. Regional geologic setting in the tectonic framework of Turkey, İAESZ: İzmir-Ankara-Erzincan Suture zone, BSZ: Bitlis Suture zone, NAFZ: North Anatolian Fault Zone, EAFZ: East Anatolian Fault Zone, GVP: Galatean Volcanic Province (Simplified from Koçyiğit, 1991); B. Location of study area in Galatean Volcanic Province in detail, empty circles indicate approximate locations of eruption centers (Modified from Geologic Map of Turkey, 1:500.000, MTA), 1: Sorgun, 2: Kavaklıdağ, 3: Daskamun, 4: Ovacık, 5: Soğuksu, 6: Köroğlu/Kartalkaya, 7: Orta volcanic complex)

Volcanic Province from Early Miocene to Pliocene (Keller, 1992; Tankut *et al.*, 1995). This magmatism is reflected in the geochemistry of volcanics by calcalkaline and alkaline associations (Öngür, 1977; Tankut and Türkmenoğlu, 1988; Tankut *et al.* 1990; Türkmenoğlu *et al.*, 1990; Türkecan *et al.*, 1991; Keller *et al.*, 1992; Tankut *et al.*, 1995). The Neogene continental deposits of the Galatean Volcanic Province is under interest for several years due to their economic resource potentials. Main Neogene lacustrine basins are Pelitçik, Güdül-Çeltikçi, Orta, Uruş, Kıbrısçık and Güvem basins (Turgut, 1978; Türkecan *et al.*, 1991; İrkeç and Gençoğlu, 1993; Tankut *et al.*, 1995). Their economic importance occur from their potential of clay minerals (especially bentonite and sepiolite), diatomites and lignite formations. The mode of occurrence of these Neogene basins are directly related with the regional geology of the Galatean Volcanic Province. Tectonism and intense volcanism are the main precursors for the formation of these economic Neogene continental lacustrine basins.

## **1.5. METHODS OF INVESTIGATION**

The methods of investigation is comprised of 4 stages in this study, Remote Sensing, Digital Elevation Model, Field and Laboratory studies.

### **1.5.1. Remote Sensing studies**

During this stage of study a Landsat 5 TM image (10.May.1991, Path 177, Row 32), which was acquired form TÜBİTAK Marmara Research

Center (Gebze) and 1:60000 scaled aerial photographs were used. The satellite image was geometrically corrected having an approximate error of 33 meters. The atmospheric effect was removed by means of radioisotopic corrections and the image was enhanced by using various image processing techniques. Several false color band combinations, band ratios and Principal Component Analysis were tried out to show the basin fill deposits and the shape of the basin. Furthermore, with the combination of processed satellite image and the existing aerial photographs a detailed geological map of the study is prepared. The data derived from aerial photographs and satellite image were fused to locate pilot areas for further detailed field studies. The most representative locations of the marginal, intermediate and central facies of the lake, the most easily accessible and the most unvegetated/uncovered areas were the ultimate criteria used in the selection of these pilot areas. All the image processing algorithms were done by using ERDAS<sup>®</sup> software on a HP-UX 700<sup>™</sup> workstation. The aerial photographs were interpreted using a stereoscope by naked eye.

### **1.5.2. Digital Elevation Model (DEM) studies**

The morphology of the study area was simulated in computer by digitizing 1:25.000 scaled topographic maps with 50 meter contours. Digital elevation model of the study area was derived to point out the relief image. Likewise the satellite image and digital elevation model of the study area are processed together to yield the 3-D view of the study area. The relief image and 3-D image were then used to interpret the morphology of the area. All

the digitizing processes were carried out with a GTCO AccuTab™ A-2 sized digitizer and ArcInfo® software. The simulation of the model is done by using ERDAS® software.

### **1.5.3. Field studies**

Field studies, under the light of remote sensing studies, were carried out during the summer period of 1995. Measurement and description of stratigraphic sections were carried out in the previously selected three pilot areas. Fresh hand specimens of 126 were collected systematically at the significant or important lithologic changes. The selection criteria of the pilot areas lead to create a combined measured section of the study area from the measured stratigraphic sections of the pilot areas. Bedding attitudes and photographs of the particular sites were taken to be interpreted in office work. Several supplementary areas at the margins of the basin were also visited to understand the stratigraphic relationships between the basin fill deposits and the surrounding volcanics.

### **1.5.4. Laboratory studies**

The laboratory part of this study is composed of petrography and mineralogy studies. A total of 45 selected representative samples were prepared for petrographic analyses, following the procedure described in Kerr (1977) for thin section preparation. For mineralogic analysis, 35 samples were pulverized for 20 seconds in the shutter-box equipment to make them pass through 200 mesh. These bulk samples were then placed on

powder packed mounts for unoriented X-ray diffraction analyses. The mounts were X-rayed at  $3^\circ 2\theta/\text{min}$  from  $2^\circ$  to  $40^\circ 2\theta$ , using Cu K $\alpha$  radiation. Standard X-ray diffraction identification procedures were applied using ASTM cards. For clay mineral analyses, the fraction smaller than  $2\mu\text{m}$  of the 23 samples out of 35 random X-rayed samples were separated and treated chemically. The chemical treatment of the samples consists of destruction of carbonates using NaOAc buffer of which pH is equal to 5. Following these treatments, smear slides of the clay fractions were prepared at air dried, ethylene glycolated, heated at  $350^\circ\text{C}$  and heated at  $550^\circ\text{C}$  conditions. All the slides were X-rayed at a scan speed of  $2^\circ 2\theta/\text{min}$  using Cu K $\alpha$  radiation. The air dried slide was scanned from  $2^\circ$  to  $30^\circ 2\theta$ , the Ethylene glycolated and heated  $300^\circ\text{C}$  slides were scanned from  $2^\circ$  to  $15^\circ 2\theta$ . Also the  $550^\circ\text{C}$  heated slide was X-rayed unless it is necessary for the identification of  $7\text{ \AA}$  minerals. Furthermore the  $d(060)$  peaks of the selected 8 clay fractions were scanned randomly to find out the di/trioctahedral structural states of the clay minerals. Scanning of random  $d(060)$  peaks were carried out in  $58^\circ$  to  $64^\circ 2\theta$  in  $1^\circ 2\theta/\text{min}$ . X-ray patterns were interpreted following the clay mineral identification methods according to Grim (1968), Carroll (1970), Pei-Yuan Chen (1977), Brindley and Brown (1980), Nemezc (1981), Wilson (1987) and Moore and Reynolds (1989). XRD analyses of the bulk rock samples were carried out in PHILLIPS PW 1729 X-ray diffractometer in Chemical Engineering Department of METU and PHILLIPS PW 3710 in MTA. The Ni filtered Cu K $\alpha$  radiation was generated by using 30 kV and 24 mA in Chemical Engineering Department and by using 40 kV and 55 mA in MTA.



The clay mineral analysis of the rock samples were done by using RIGAKU Geigerflex in MTA with 40 kV and 30 mA. The details of XRD sample preparation stage is presented in Appendix A.

In addition to the XRD studies 8 samples were selected for Fourier Transform Infrared analyses in Chemistry Department of METU using Mattson 1100 FTIR Spectrometer. The sample preparation stage is described in Appendix B.

Also 10 samples were selected to study the morphology of the clay minerals, associated non-clay minerals and the precursors, with Scanning Electron Microscope in Metallurgical Engineering Department of METU using JEOL JSM-6400 Scanning Electron Microscope and its associated EDX.

## CHAPTER 2

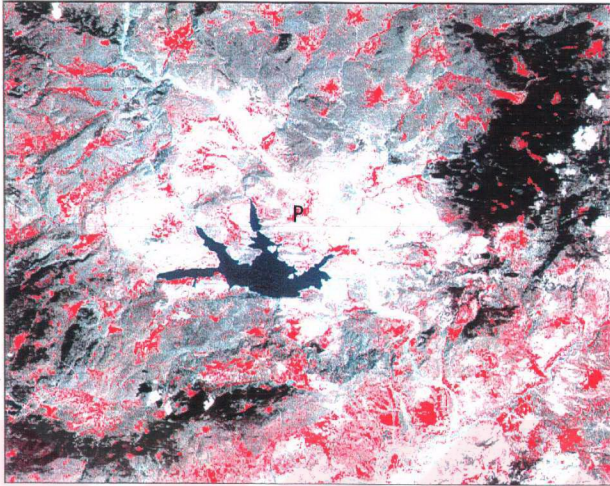
### GEOLOGY

#### 2.1. GENERAL GEOLOGY

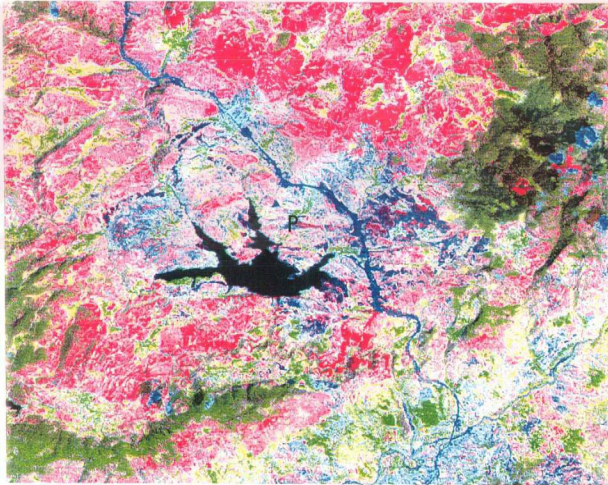
Pelitçik Basin is the greatest Neogene lacustrine basin of the Galatean Volcanic Province. The basin is located in the south central part of the province. This Neogene lacustrine basin is surrounded by volcanics of Galatean Province in every directions (Figure 2.1). The remote sensing studies show that the basin has an ellipsoidal shape with a length of 20 km and a width of 12 km (Figures 2.1 and 2.2.a, b). The basin fill deposits which have high reflectance appears as white in all of the single bands of Landsat 5. The most perceptible view of the basin is encountered in the false color composite as white (where band assignments are red=4<sup>th</sup>, green=3<sup>rd</sup> and blue=2<sup>nd</sup> band of Landsat 5 TM, Figure 2.2.a) and as blue in pseudo color composite after Principal Components Analysis (PCA) (where band assignments are red=1<sup>st</sup>, green=2<sup>nd</sup>, blue=3<sup>rd</sup> after PCA, Figure 2.2.b). The basin represents a topographically low area bounded by high volcanic terrain (Figures 2.3 and 2.4) and is separated from Çeltikçi graben by a NE-SW trending horst (Figure 2.4.). The drainage pattern in the study area and vicinity is composed of dendritic to trellis drainage pattern, in which the flow direction is all to the south, to the Çamlıdere Dam reservoir (Figure 2.5).



**Figure 2.1.:** Geologic map of the study area. (1: Quaternary Alluvium; 2: Mio-Pliocene Pazar Formation; 3: Galatean volcanics; 4: Fault; 5: Strike and Dip Direction; 6: Location of Measured Stratigraphic Sections; A-A': Yoncatepe Measured Section; B-B': Buğrular Measured Section; C-C': Akkayatepe Measured Section.



A



B

**Figure 2.2.:** Landsat 5 TM image of the study area, A) False color composite (Red=4, Green=3, Blue=2), B) Pseudo color composite after PCA analysis. Base line of the images are approximately 40 km, the images are in true north orientation (P=Pelitçik village).

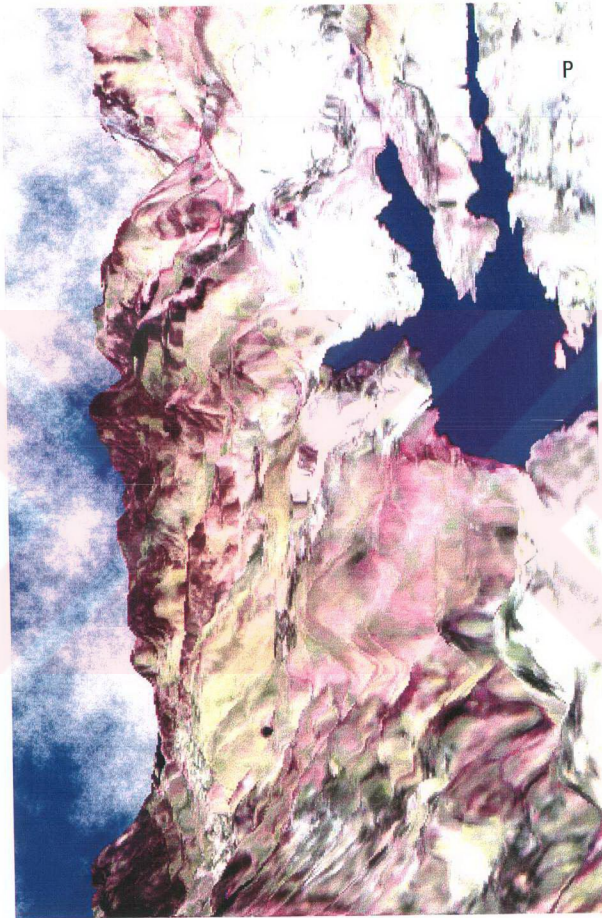


**Figure 2.3.:** 3-dimensional view of the study area based on Landsat False Color (Red=7, Green=5, Blue=3) composite. View is from east to west (P=Pelitçik village).

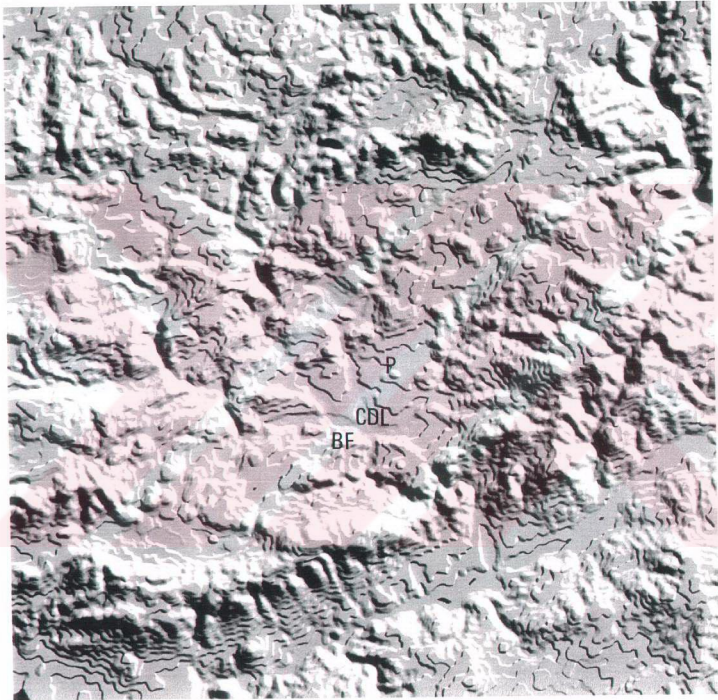


**Figure 2.4.:** Relief image of the study area and its vicinity, base line of the image is 44 km and image is in true north orientation (P=Pelitçik village, ÇDL=Çamlıdere Dam Lake, BF=Bayındır Fault).

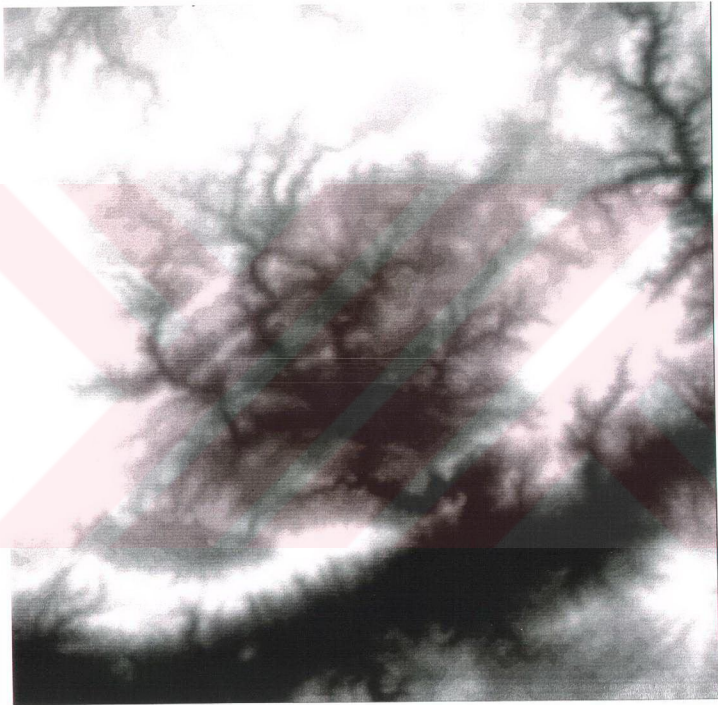


**Figure 2.5.:** Digital Elevation Model of the study area and its vicinity. Dark areas show low topography, lighter areas show higher topography. The base line of the image is 44 km and the image is in true north orientation (P=Petitçik village).

The basin fill deposits of Pelitçik basin is represented by Pazar formation. The bedding attitudes of Pazar formation follow the shape of the basin except the southern margin, in which the basin is truncated by the Bayındır fault (Figures 2.1, 2.2.a, 2.2.b, 2.4 and 2.6). The dip directions of Pazar formation are all to the south in the study area. The Pazar Formation conformably overlies the Galatean volcanics. The generalized columnar section of the Pelitçik basin starts with Galatean volcanics having andesitic-dacitic composition at the bottom. The lacustrine facies involves several tuff layers and lens shaped volcanoclastic deposits. General lithologies observed in this sequence are mudstone with thin coal horizons, claystones and dolomicrites (marls). At the top of the section alluvium unconformably overlies the lacustrine facies (Figure 2.7).





**Figure 2.6.:** Field view of the Bayındır fault scarp. View is from north to south (BF=Bayındır Fault).

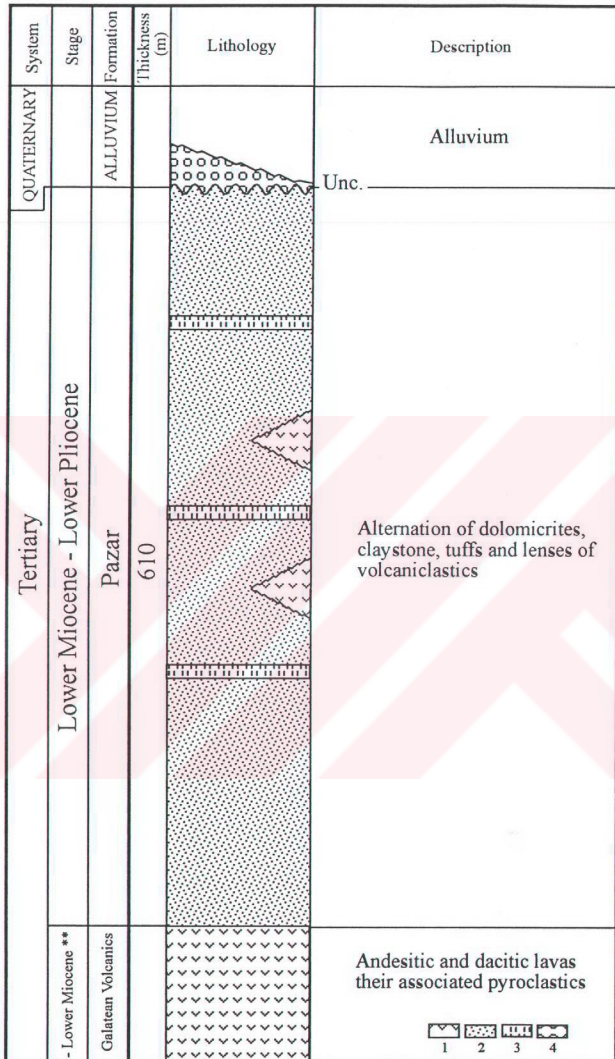


**Figure 2.7.:** Generalized stratigraphic section of the Pelitçik Basin; 1:Galatean Volcanics; 2: Lacustrine facies; 3: Tuff layers; 4: Alluvium; \*\*: in the study area.

## **2.2. STRATIGRAPHY**

The Neogene stratigraphic sequence of the study area is composed mainly of two groups: i) the Galatean volcanics and ii) Pazar formation.

### **2.2.1. Galatean volcanics**

#### **2.2.1.1. General Definition**

Galatean volcanics of the study area are composed mainly of andesites, basaltic andesites and their associated volcanic units. Various names are given to these volcanics, of the Galatean Volcanic Province, such as Tertiary Volcanic Series by Erol (1955); K ro glu Volcanic Complex by Ketin (1966, 1977) and Tankut *et al.* (1990); AA lavas, Intermediate lavas and Lahar by  nl  (1973); Lower, Intermediate, Upper Lavas and Pyroclastic products by Tatlı (1975); Lower, Binkoz, Karalar and Tekke lavas, Volcanic Breccia and Lahar by  ng r (1976, 1977); and Karasivri, Kirazdađı, Ilıcadere, Deve ren and Bakacaktepe volcanics by T rkecan *et al.* (1991). The above given names are either in very general sense or overlapping each other in a very local manner, so to carry the confidentiality and to avoid the misleading in the literature, volcanics and their associated rocks are referred to as “Galatean volcanics” in the study area.

#### **2.2.1.2. Distribution and boundaries**

Galatean volcanics comprise the basement of the study area and show extensive outcrops. There are five eruptive complexes in the vicinity of the study area (Figure 1.2): Kızılcahamam (Sođuksu) complex in the east, Ovacık complex in the north, Daskamun in the northwest and Kavaklıdađ in

the west (Tankut *et al.*, 1995). In addition, another volcanic complex (Sorgun) in southwest is proposed. The base of Galatean volcanics could not be seen in the study area. Galatean volcanics are overlain conformably with the Pazar formation.

### 2.2.1.3. Lithology

Galatean volcanics exhibit very diverse lithologies, so only the distinct properties will be mentioned. They are composed mainly of three types, lavas, pyroclastics and volcanoclastic deposits.

Lavas are generally brown to brick red in color and their composition ranges from andesite to basaltic andesite.

The pyroclastics are white to cream or gray in color and do not have extensive outcrops. The largest outcrop of the pyroclastics is observed in the vicinity of Sarikavak village (Figure 2.8). This outcrop, embedded in the volcanoclastic deposits, is rich in ash and pumice particles, which suggests to a single, subaerial eruption (Schumacher, 1995; personal communication). Apart from this particular outcrop, nine different tuff layers were identified in the three measured stratigraphic sections of the Pazar formation, which will be discussed in section 2.2.2.. Among these tuff layers, one significant tuff layer, which shows an accretionary lapilli character (Fisher and Schminke, 1984; Schumacher, 1995; personal communication), was identified near Yoncatepe village.

The components of volcanoclastic deposits are lithologically similar to the previously mentioned lavas and pyroclastics (Figure 2.9). It contains brick red to brown andesitic, gray dacitic and black glassy blocks of various sizes, in which their size ranges from few centimeters to few meters. These



**Figure 2.8.:** Field view of Sarıkavak Tuff (Location: S of Sarıkavak village).



**Figure 2.9.:** Field view of volcaniclastic deposits (Location: West of Yoncatepe village).

volcaniclastics are very thick bedded but they seem to be massive when they are examined in single particular beds. The dominant rock types of these volcaniclastic deposits are lavas, tuffs and fluvial clastics. These fluvial clastics are medium bedded and locally exhibit cross bedding (Figure 2.10).



**Figure 2.10.:** Cross bedding in the upper parts of volcaniclastic deposits.

Numerous volcaniclastic lenses are observed within the basinfill deposits. They are generally elongated mostly in the NE-SW and E-W directions, parallel to the strikes of lacustrine beds. The volcaniclastic lenses generally pinchout towards south and no volcaniclastic lenses are observed in the southern parts of the basin. On the other hand, presence of crossbeddings in the volcaniclastics suggests exists a high energy fluvial

environment near to the shores of the lake, in the spasmodic activities of volcanism and/or tectonism. The same situation is also valid for the generation of volcanoclastic lenses in the basin.

#### **2.2.1.4. Age**

Based on previous studies, the age of Kavaklıdağ, Daskamun and Ovacık volcanic complexes is assigned as Early Miocene (Türkecan *et al.*, 1991; Keller *et al.*, 1992; Tankut *et al.*, 1995). No age determinations were available for Soğuksu complex in the literature, but based on their stratigraphic position, an age of Early Miocene can be assigned.

### **2.2.2. Pazar formation**

#### **2.2.2.1. General Definition**

The Pazar formation was first named by Tatlı (1975). The name of this formation come from the biggest village which is located outside the study area at the east of Kızılcahamam. Pazar formation consists of alternations of gray-green claystones, white argillaceous dolomicrites, cherty white limestones, white to pink limestones, several tuff layers and minor coal occurrences. In the middle sections of the Pazar formation some lenses of volcanoclastic deposits are also observed.

### **2.2.2.2. Distribution, Boundaries and Thickness**

The Pazar formation is located in the central part of the study area and surrounded by Galatean volcanics in all directions. The Pazar formation conformably overlies the Galatean volcanics. The upper boundary of the Pazar formation is represented by an erosive contact with the Quaternary alluviums. The total combined measured thickness of the Pazar formation is found to be 610 meters (Figure 2.7)

### **2.2.2.3. Lithology**

Because of the structural discontinuities three pilot areas were chosen to study and construct a combined measured stratigraphic sections of the Pazar formation. These are referred to as Yoncatepe (A-A'), Buğralar (B-B') and Akkayatepe (C-C') sections (Figure 2.1)

The Yoncatepe section (Figures 2.1, 2.11 and 2.12), which is representing the shore facies of the lacustrine deposits, starts with a volcanoclastic deposit at the base. This volcanoclastic deposit consists of a sand sized matrix and andesitic-dacitic and black glassy blocks. It has a bedding attitude of N45°E and a dip amount of 15° to S. The accretionary lapilli layer is located in the uppermost parts of this volcanoclastic deposit, having a thickness of 2 meters. Immediately after the volcanoclastics a crystal-vitric tuff layer of 8.3 meters is encountered. This is followed by a 5



Figure 2.11.: Measured Stratigraphic Section of Yoncatepe Sequence (1: argillaceous dolomitic, 2: claystone, 3: dolomite, 4: tuff, 5: cherty limestone, 6: volcaniclastics, 7: accretionary lapilli)

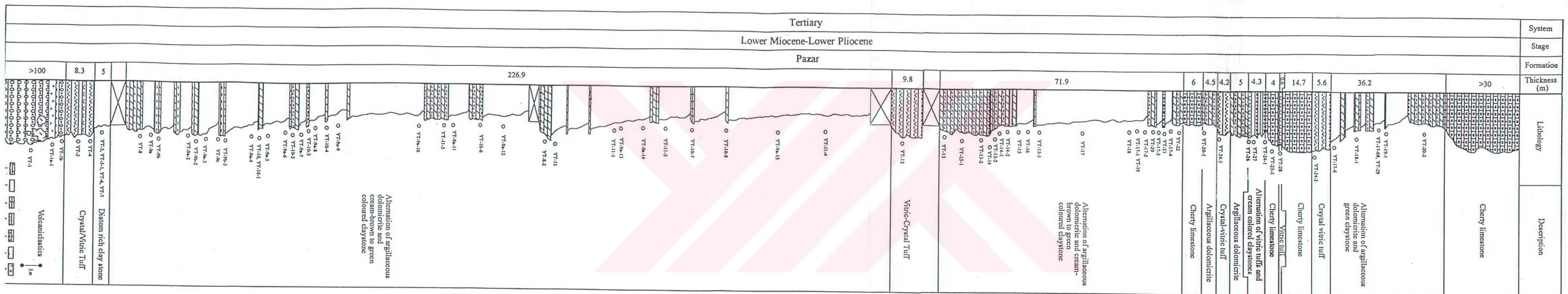




**Figure 2.12.:** Location of Yoncatepe Measured Stratigraphic Section, looking in northwest direction (Village seen at the left corner is Yoncatepe village).

meters thick diatom rich claystone. Above this diatom rich claystone, 226.9 meters thick, lithology consists of alternation of very thin bedded white argillaceous dolomicrite and cream-brown to green, non bedded claystone is measured. This zone is disrupted with the presence of another white to gray, thin to medium bedded, pumice rich, vitric-crystal tuff layer of 9.8 meter thick. This tuff horizon is followed by a 71.9 meters of alternation of argillaceous dolomicrite and cream-brown to green claystones same as below this tuff layer. Going upwards in the measured section, a zone, starting with cherty limestone and ending with a crystal vitric tuff (Sample

no YT-24-02) comes, which is the most complicated part in this section. This zone is composed of alternations of medium bedded cherty limestones, thin bedded argillaceous dolomicrites, four separate layers of thin bedded tuffs and nonbedded cream claystone. This zone comprises 49.4 meters of the measured sequence. The sequence is again encountered as the alternation of argillaceous dolomicrite and green claystone of 36.2 meters thick. Finally, the Yoncatepe section ends up with cherty limestone of 30 meters thick. At some other locations, stratigraphically equivalent of Yoncatepe section, some minor coal or organic rich claystones are observed.

Buğralar section (Figures 2.1, 2.13 and 2.14) represents slightly deeper facies of the lacustrine deposits and starts with a lens shaped volcanoclastic deposit (Figures 2.1 and 2.15) similar to the volcanoclastic deposits of Yoncatepe section. This unit has an apparent thickness of greater than 70 meters. The section continues about 17.5 meters with alternation of gray, green, brown claystones, in which zones of silicified woods are observed. A zone of 15.4 meters in the section is seen as the alternation of green claystones, black organic rich shales and a few meters thick black chert bands. The distinctive lithology of this 15.4 meter thick zone is the 5.2 meters thick crystal-vitric tuff layer. The remaining 15 meters of this measured section is composed of alternation of white medium bedded argillaceous dolomicrites, white to gray dolomicrites and nonbedded green-gray claystones having some thin coal seams.

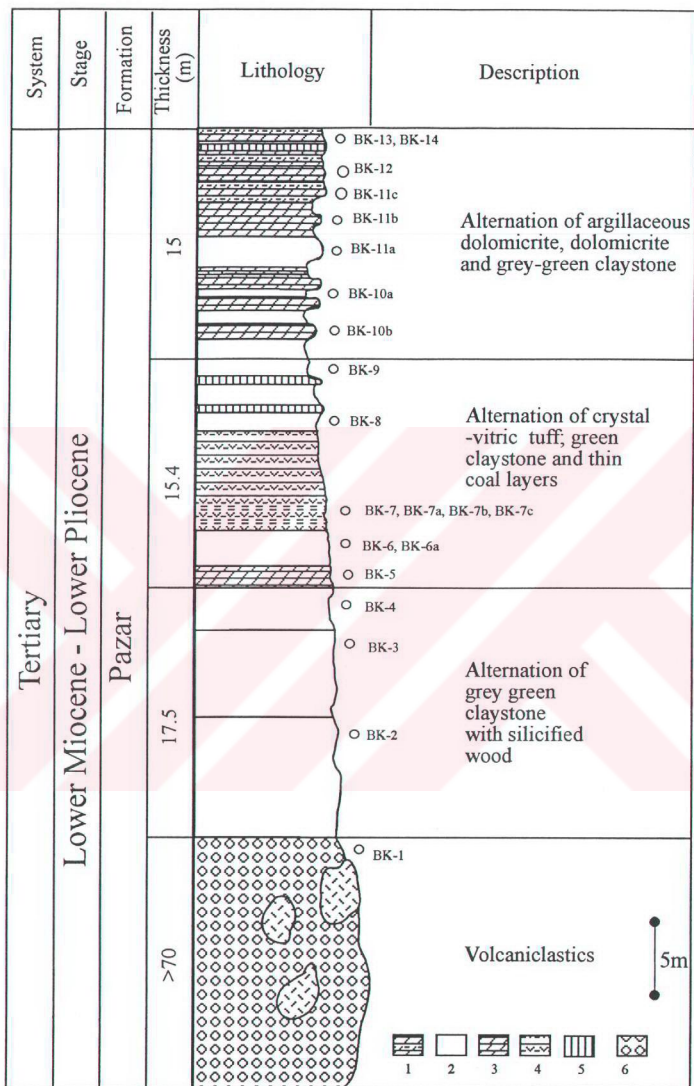


**Figure 2.13.:** Measured Stratigraphic Section of Buğralar Sequence (1: argillaceous dolomicrite, 2: claystone, 3: dolomicrite, 4: tuff, 5: chert, 6: volcaniclastics).



**Figure 2.14.:** Field view of Buğralar Measured Stratigraphic sequence



**Figure 2.15.:** Volcaniclastic lens at the base of Buğralar sequence  
(Location: northeast of Buğralar village).

Akkayatepe section (Figures 2.1, 2.16 and 2.17), the deepest facies of the lacustrine sequence, starts with 59.9 meters of alternation of white dolomicrites, gray green dolomite rich claystones. Following in the section a distinctive zone of 1.8 meters with analcime rich gray to gray-green mudstone layer is encountered. The section continues with a dolomicrite and white crystal vitric tuff layers, having thickness of 3.3 meters and 8.6 meters, respectively. Above it alternation of white argillaceous dolomicrites and medium bedded limestones with solution cavities are measured for about 39 meters. Another vitric tuff layer of 2.5 meters thick is measured before 2 meters of black chert layer. Finally 3 meters of Ostracoda and Pelecypoda rich limestone is measured in the Akkayatepe measured section.

#### **2.2.2.4. Age**

The age of the Pazar formation is determined through radioisotopic dating of the surrounding volcanics and palynological data from the organic rich beds of the basin. According to palynological studies, an age of Middle Miocene is given from Çeltikçi basin which is thought to be in contact with Pelitçik basin in mature stages (Turgut, 1978); moreover, an age of Early Miocene is attributed also from the palynomorphs from Osmansın area located at the western part of the basin (Türkecan *et al.*, 1991). Based on these palynologic data and radioisotopic age determinations of volcanics in

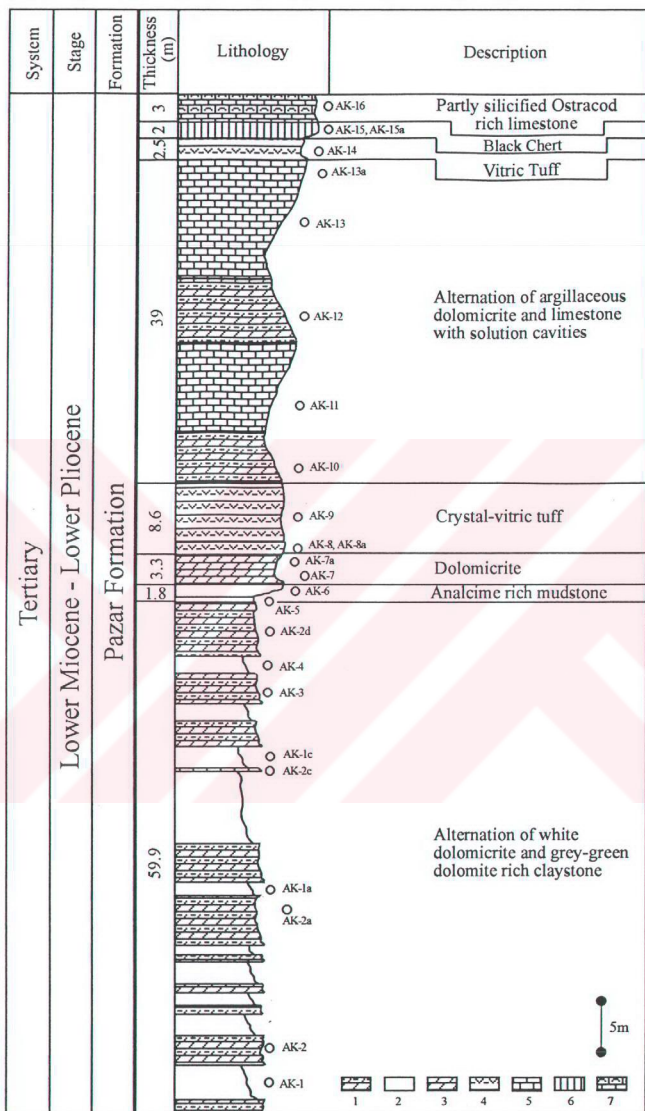


**Figure 2.16.:** Measured Stratigraphic Section of Akkayatepe Sequence (1: argillaceous dolomiticrite, 2: claystone, 3: dolomiticrite, 4: tuff, 5: limestone, 6: chert, 7: Ostracod rich limestone)



**Figure 2.17.:** Field view of Akkayatepe measure stratigraphic sequence. (Location: southeast of Buğralar village, B=Buğralar village).

the study area, Tankut *et al.* (1995) stated that the deposition of Pazar formation should have been started in Early-Middle Miocene and continued in Pliocene.

### **2.2.3. Quaternary Alluvium**

Alluvium is composed of clay to sand sized material derived from the bedrock in the area, and deposited in or near the stream channels (Figure 2.1).



## **CHAPTER 3**

### **MINERALOGY**

The mineralogical and petrographical properties of the Pazar formation are studied by means of an optical microscope, X-ray diffraction analysis (XRD), scanning electron microscope (SEM) equipped with Energy Dispersive X-Ray Analysis (EDX) system and Fourier Transform infrared Spectroscopy (FTIR) methods. The mineralogy and petrography of whole-rock and clay mineral fraction of Pazar formation is presented in this chapter.

#### **3.1. THIN SECTION STUDIES**

A total of The representative 45 thin sections of lacustrine facies, out of 126, of systematically collected samples were selected to study the mineralogical and petrographical properties of the Pazar formation. The purpose of thin section studies is to investigate in detail the petrography of lithologies that were identified in field studies, to define non-clay

mineralogy and to select samples for X-ray diffraction, Scanning Electron Microscope and Fourier Transform Infrared Radiation analyses.

### 3.1.1. Yoncatepe Section

The Yoncatepe measured section of the Pazar formation contains 7 well distinguished tuff layers (Figure 2.11). The most outstanding layer among these tuff layers is the accretionary lapilli zone (Schumacher, 1995; personal communication) This zone is located at the base of the section, embedded in the uppermost levels of the volcanoclastics (Sample No: YT-1a-1, Figure 2.11). The core of this lapilli is coated by a number of relatively fine grained and iron oxidized rims (Figure 3.1). The type of the accretionary lapilli is determined as Multiple Rim Accretionary Lapilli (Schumacher and Schminke, 1991, 1995).

Antithetically, the other tuff layers are classified as lapilli tuff, pumice rich lapilli tuff, vitric tuff and crystal vitric tuff. The feldspars (Figure 3.2), quartz, volcanic rock fragments (Figure 3.2), pumice fragments (Figure 3.3), glass shards (Figure 3.4) and biotite are the major constituents of these tuffs. The clay minerals either constitute the matrix or seen as alteration products.

The rest of the Yoncatepe section is consisted primarily of claystones, argillaceous dolomicrites and cherty limestones. The mineralogy of the claystones is evaluated by X-ray diffraction techniques which will be

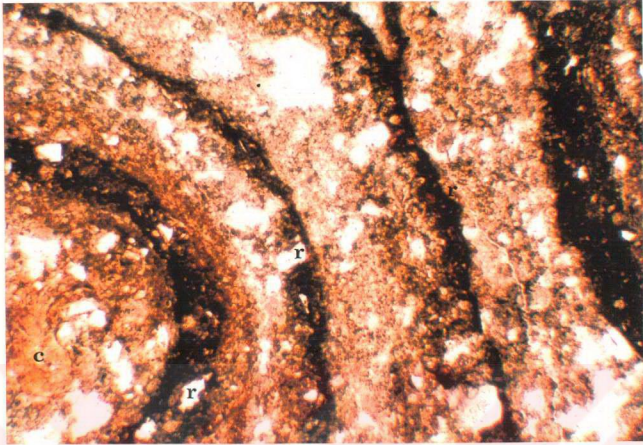


**Figure 3.1.:** Photomicrograph showing Multiple Rim Accretionary Lapilli, (r) rim, (c) core, (Sample No: YT-1-a1, Mag. X45, PPL)

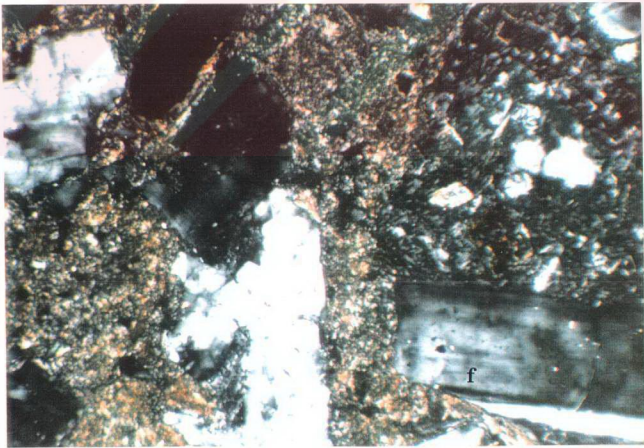


**Figure 3.2.:** Photomicrograph showing feldspars (f) and volcanic rock fragments in crystal vitric tuff (Sample No: YT-24-01, Mag. X170, XPL)

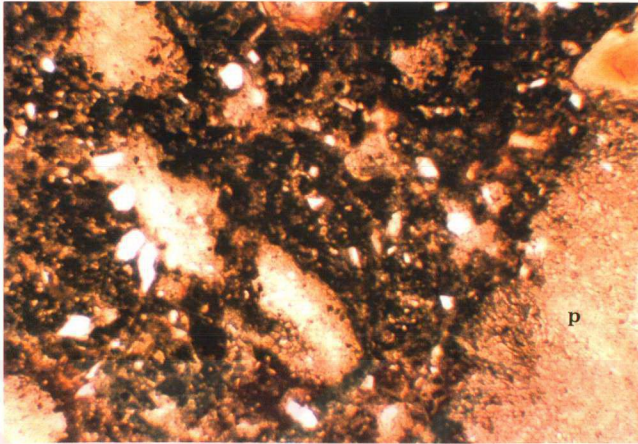


**Figure 3.3.:** Photomicrograph showing pumice fragments (p) in vitric tuff, (Sample No: YT-4, Mag. X45, PPL)

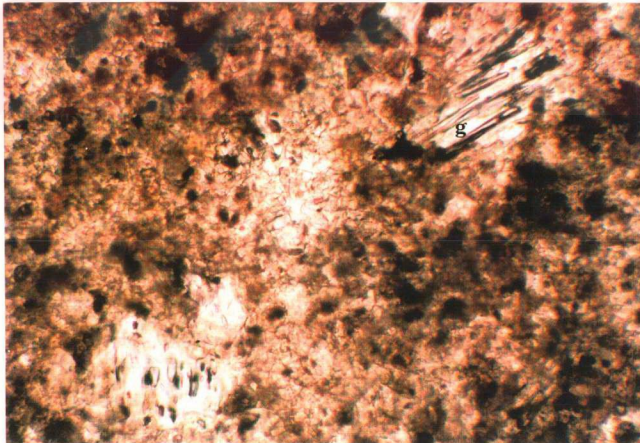


**Figure 3.4.:** Photomicrograph showing glass shards (g) vitric tuff (Sample No: YT-26, Mag. X170, PPL)

discussed later in this chapter. However, in the lowermost parts of the claystone facies, a particular zone rich in siliceous shell bearing organisms (Diatomacea ?) (Altner,D., 1996; personal communication) is encountered in the thin sections of the Yoncatepe measured section (Figure 3.5).

In the argillaceous dolomicrite facies, generally the matrix is composed of various clay minerals. Furthermore, the major constituent of this facies is found to be finely crystalline dolomite rhombs (micro dolomites) which are floating over the matrix, mica flakes and iron concentrations that are embedded in the previously mentioned clayey matrix (Figures 3.6 and 3.7). This floating habit of dolomite rhombs indicate a diagenetic history, in which the crystal dimensions of dolomite rhombs increase. This phenomenon will be discussed in detail in the dolomite stoichiometry section further in this chapter.

In the top most levels of the Yoncatepe section the cherty limestone facies is mostly composed of black chert nodules and clasts of argillaceous dolomicrites, which are cemented by calcite or locally by aragonite (Figure 3.8).

### **3.1.2. Buğralar Section**

This short subsection of the measured Pazar formation consists of three zones: i) claystone facies with silicified woods, ii) alternation of crystal vitric tuff and claystone with thin coal layers, and iii) alternation of argillaceous dolomicrite and claystones (Figure 2.13).

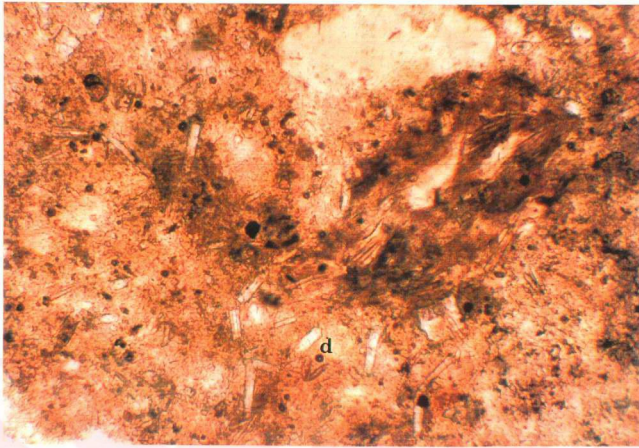


**Figure 3.5.:** Photomicrograph showing siliceous shell bearing organisms (Diatomacea ?) in claystone, (d) Diatomacea, (Sample No: YT-7, Mag. X170, PPL)

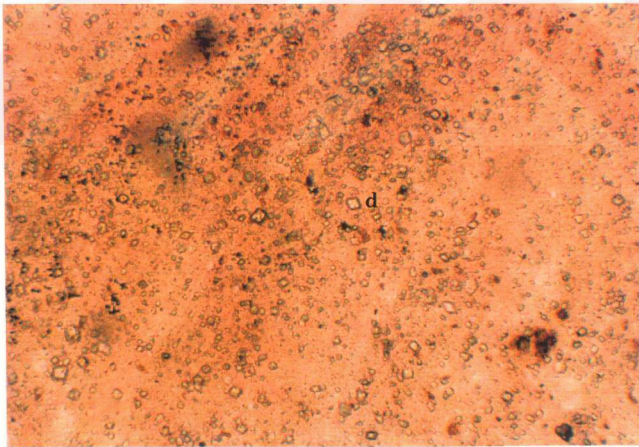


**Figure 3.6.:** Photomicrograph showing dolomicrite rhombs in argillaceous dolomicrites, (d) dolomite, (Sample No: YT-10-03, Mag. X170, PPL)

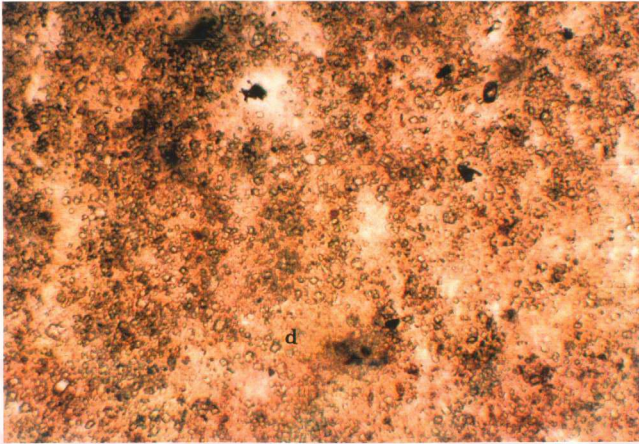


**Figure 3.7.:** Photomicrograph showing dolomicrite rhombs in argillaceous dolomicrites, (d) dolomite, (Sample No: YT-18-01, Mag. X170, PPL)



**Figure 3.8.:** Photomicrograph showing the aragonite cement of cherty limestone facies, (a) Aragonite, (Sample No: YT-25-01, Mag. X45, XPL)

Tuff layers in this section contain enough glass shards and crystal fragments to classify them as crystal-vitric tuff. In the argillaceous dolomicrites a clay rich matrix embeds the micro dolomite rhombs, which are smaller than those of the Yoncatepe section and can hardly be seen under plane polarized microscope (Figure 3.9). Also another difference of this argillaceous dolomicrite facies from its Yoncatepe equivalent, is the presence of minor gypsum veins in few samples (Figure 3.10).

### **3.1.3. Akkayatepe section**

Similar to the Yoncatepe and Buğralar sections, Akkayatepe section is mainly dominated by the alternation of argillaceous dolomicrites (Figure 2.16) and claystones. Two significant tuff layers are encountered in this section, as crystal-vitric (Figure 3.11) and vitric tuffs (Figure 3.12).

At the upper levels of this section the alternation of argillaceous dolomicrites and limestones are measured. The amount of clayey matrix in the argillaceous dolomicrites is much more abundant than the equivalent facies of the Buğralar and Yoncatepe measured sections (Figure 3.13). In addition, the dolomite rhombs do not exhibit a floating manner but they are seen as embedded in the matrix, which may be an indication of primary crystallization. Furthermore their size relations with respect to their chemistries will be given in dolomite stoichiometry section later in this chapter.



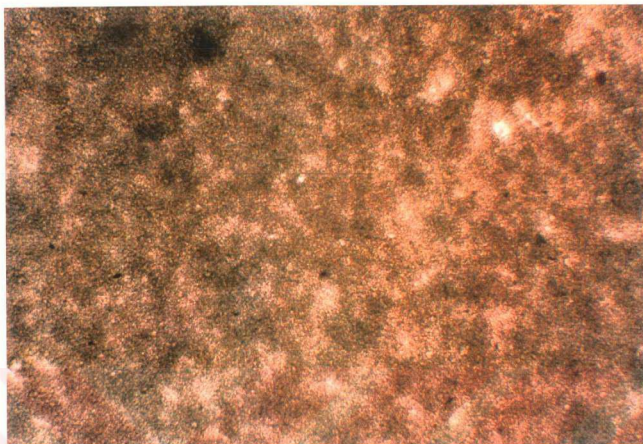


**Figure 3.9.:** Photomicrograph showing the microdolomite rhombs embedded in clayey matrix, (Sample No: BK-10b, Mag. X170, PPL)

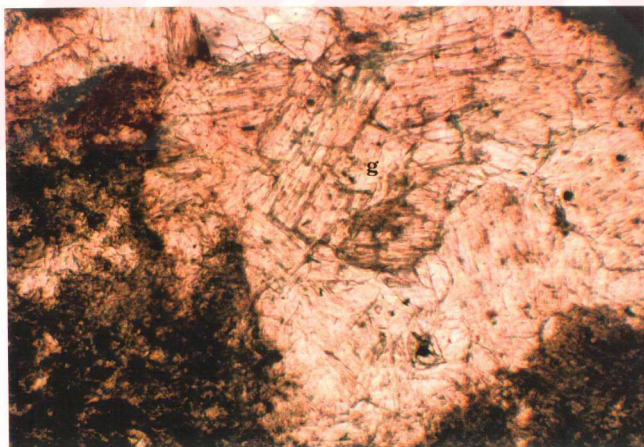


**Figure 3.10.:** Photomicrograph showing the gypsum vein in argillaceous dolomitic facies. (g) gypsum, (Sample No: BK-11b, Mag. X170, PPL)

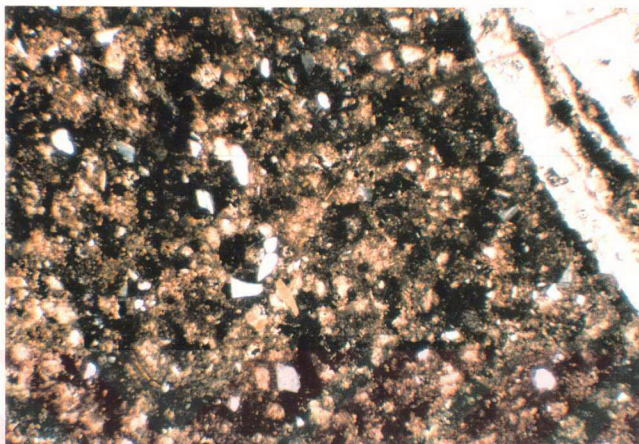


**Figure 3.11.:** Photomicrograph showing the general view of the crystal vitric tuff, (Sample No: AK-8, Mag. X45, XPL)

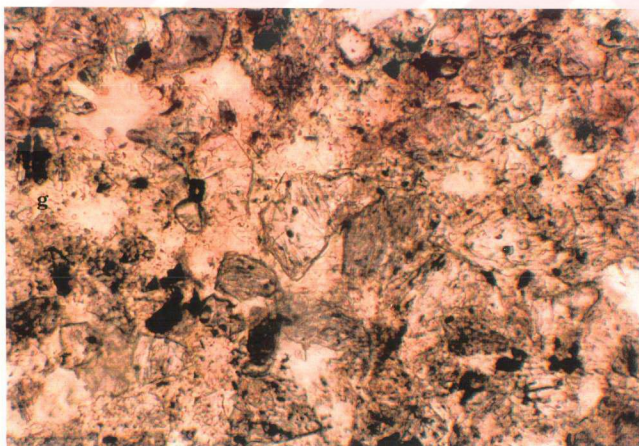


**Figure 3.12.:** Photomicrograph showing the general view of vitric tuff (g) glass shard, (Sample No: AK-9, Mag. X170, PPL)

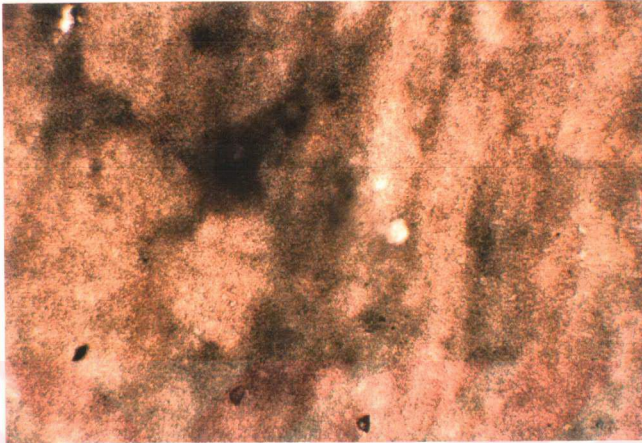


**Figure 3.13.:** Photomicrograph showing the general view of argillaceous dolomiticrite facies, (Sample No: AK-10, Mag. X45, PPL)

On the other hand the limestones have significant solution cavities, seen in hand specimens. The walls of these caves are lined with calcite crystals perpendicular to the surface. The calcite crystals, precipitated on the walls of these solution cavities exhibit a vadose environment for diagenesis (Figure 3.14).

The analcime crystals in the analcime rich mudstone are very fine to observe in the polarized microscopes, so they are going to be mentioned in X-ray diffraction studies and Scanning Electron Microscope studies.

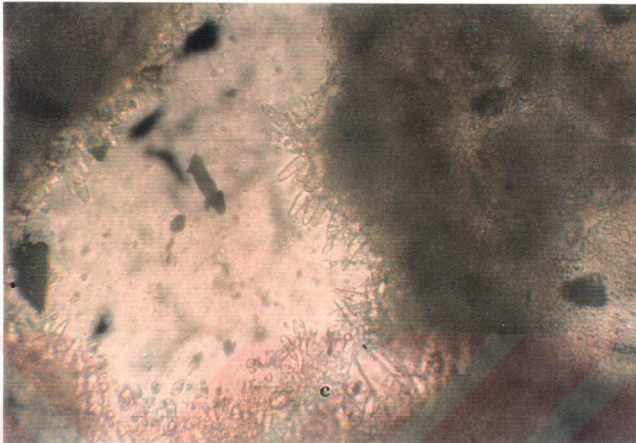


**Figure 3.14.:** Photomicrograph showing the calcite (c) precipitation in the walls of solution cavities, (Sample No: AK-13a, Mag. X430, PPL)

## **3.2. X-RAY DIFFRACTION STUDIES**

The X-ray diffraction analyses are performed to assess the non-clay mineralogy and types of clay minerals of the Pazar formation. The d-spacing values of the studied minerals of Pazar formation is given in Appendix C.

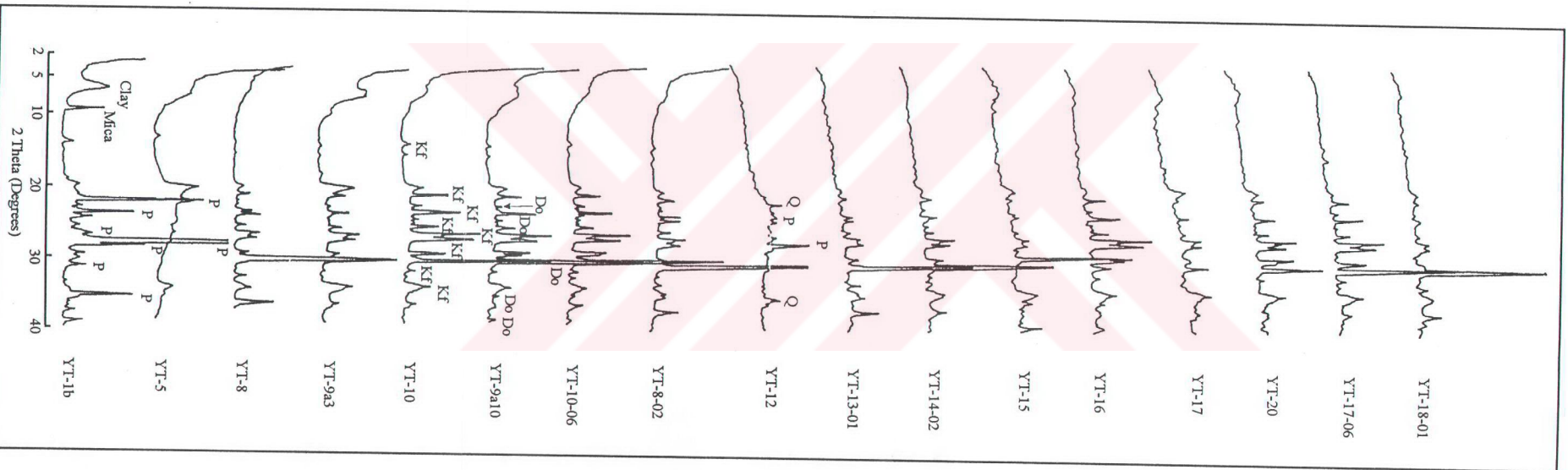
### **3.2.1. Non-clay Mineralogy**

In order to determine the non-clay mineralogy of Pazar formation 35 samples were selected out of 126 collected samples on the basis of thin

section studies. The selected samples were pulverized to pass through 175 mesh sieve. Samples were than X-rayed randomly on powder packed mounts within the range of  $2^{\circ}$  to  $40^{\circ} 2\theta$  at a scan speed of  $3^{\circ} 2\theta/\text{min}$ , using Cu K $\alpha$  radiation and Ni filter.

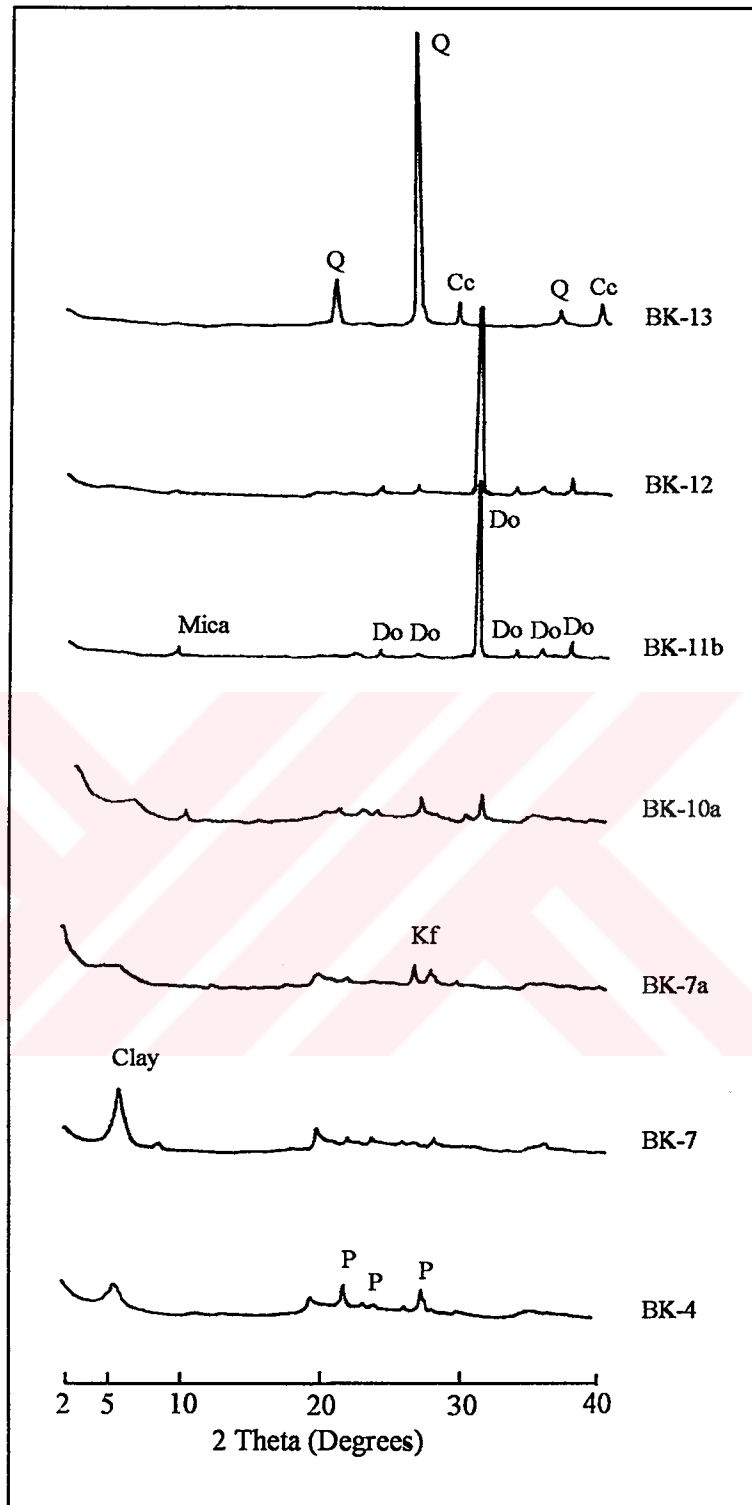
The mineralogy of whole-rock fraction of the Yoncatepe section is carried out on selected 18 representative samples. Generally all of the samples have dolomite, K-feldspar and/or calcite peaks. Furthermore, the peaks belonging to clay minerals is hardly be seen in the X-ray diffraction patterns of randomly oriented mounts of the whole rock samples (Figure 3.15). Nevertheless, three samples disclose to the formerly mentioned situation, which are taken from volcanoclastic base (Sample No: YT-1-b), siliceous shell bearing organism (Diatomacea ?) rich claystone (Sample No: YT-5) and vitric tuff (Sample No: YT-12). The sample taken from volcanoclastic base has all of the peaks of plagioclase group minerals in the  $2^{\circ}$  to  $40^{\circ} 2\theta$  range. Moreover the clay fraction of this sample is overestimated and show the sharpest peaks of this section. The Diatomacea (?) rich claystone sample exhibits an X-ray diffraction pattern similar to amorphous silica around  $4\text{\AA}$ , which supports the presence of siliceous shell bearing organisms in the sample. The tuff sample (YT-12) shows quartz and plagioclase peaks which once more support the petrography studies.

Figure 3.15: X-ray diffraction patterns of unoriented whole-rock samples of Yoncatepe sequence.



The mineralogy of whole-rock fraction of the Buğralar section is carried out on selected 7 representative samples. The X-ray diffraction patterns of this sequence starts with plagioclases associated with clays and micas, following the sequence upwards plagioclases turn into K-feldspars again associated with clays and micas (Figure 3.16). The overall crystal intensities of the above mentioned samples are lower than those of samples in the Yoncatepe sequence. However, the samples BK-11b and BK-12 are the typical examples of dolomicrite facies exhibiting intensely all the characteristic peaks of dolomite in  $2^{\circ}$  to  $40^{\circ}$   $2\theta$  range.

The mineralogy of whole-rock fraction of the Akkayatepe section is carried out on selected 8 representative samples. The sequence is generally represented as the association of clays, K-feldspars and dolomites in the whole rock XRD patterns. The main difference of the XRD patterns of this sequence apart from other sequences is the presence of analcime peaks in two samples (Sample No: AK-5, AK-6; Figure 3.17).



**Figure 3.16.:** X-ray diffraction patterns of unoriented whole-rock samples of Buğralar sequence



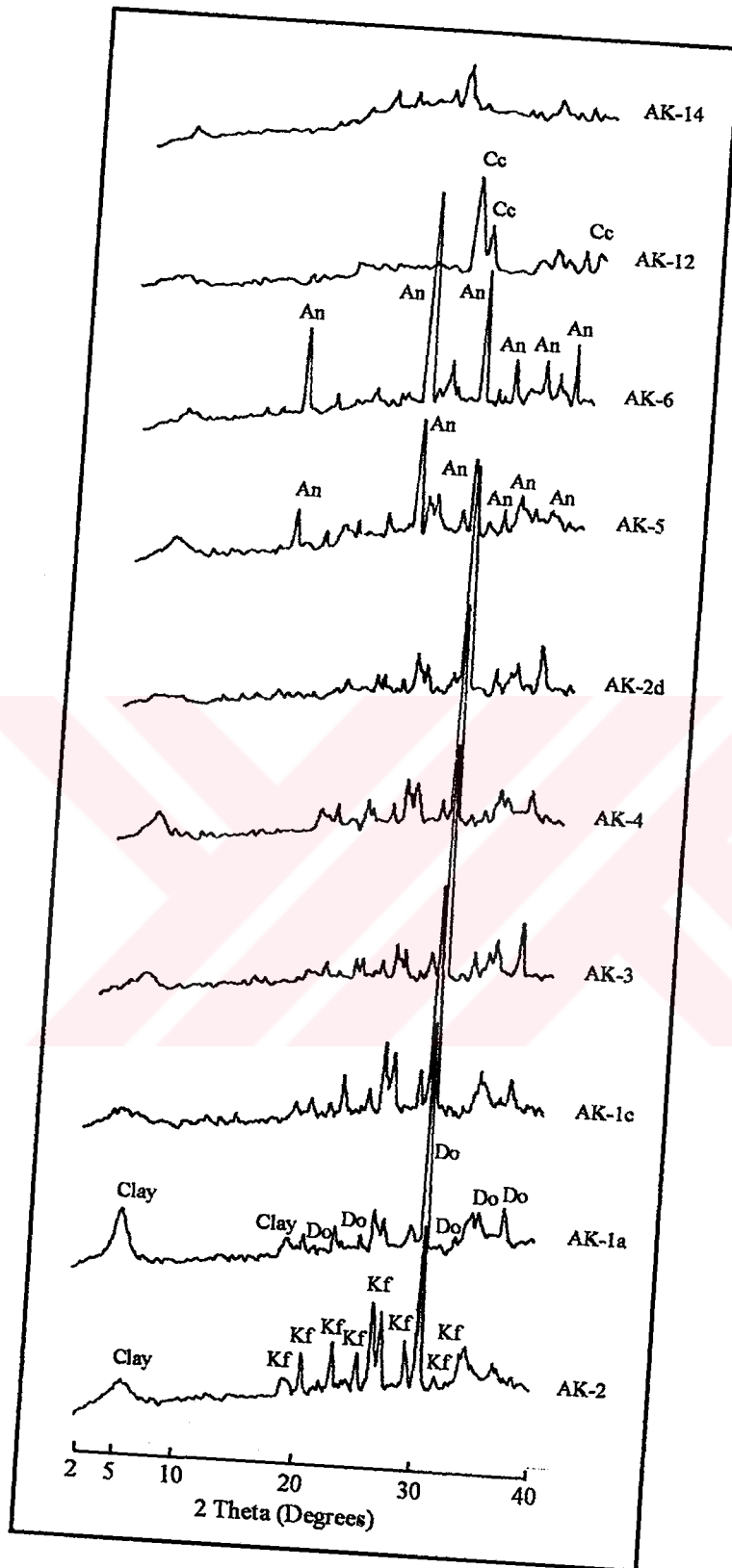


Figure 3.17.: X-ray diffraction patterns of unoriented whole-rock samples of Akkayatepe sequence.

### 3.2.2. Dolomite Stoichiometry

The mineral dolomite is stoichiometric in ideal, but never occurs as stoichiometric in nature. This non-stoichiometric character of dolomites give important clues for the geochemistry of their depositional environment.

A total of 26 samples of the Pazar formation contain various amounts of dolomites with varying chemistry as indicated by the variations of  $d$  (104) peaks in XRD patterns. The Ca excess of the dolomites of the Pazar formation are calculated according to the following formulae given in Lumsden (1979).

$$N_{CaCo_3} = M * d + B$$

Where  $M = 333.33$ ,  $B = -911.99$  and  $d$  is equal to the  $d$  (104) peak of the dolomite (Figure 3.18). Likewise the ordering ratio of the dolomites indicate whether the dolomites are products of primary precipitation or not. All the naturally occurring dolomites are ordered to an extent (otherwise the mineral is not dolomite strictly) with most modern dolomites showing poor ordering reflections compared with many ancient dolomites. The degree of ordering is determined by the following ratio (Goldsmith and Graf, 1958 a,b).

$$\text{Degree of ordering} = \frac{\text{Intensity of 015 peak}}{\text{Intensity of 110 peak}}$$

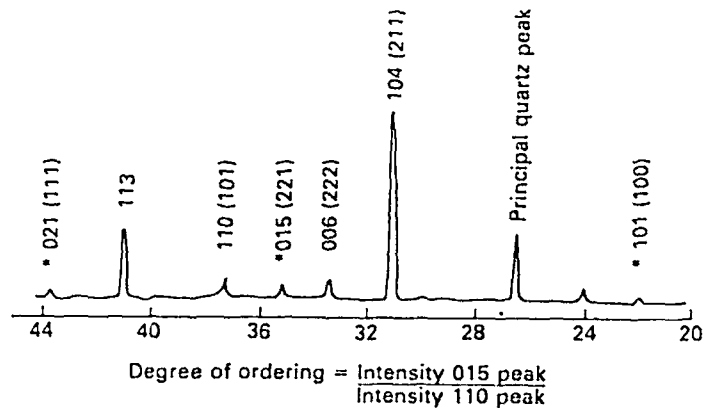


**Figure 3.18.:** The X-ray diffraction peaks of dolomite (Hardy and Tucker, 1988).

After the previously mentioned analyses are carried out, the dolomites of Pazar formation are found to be non-stoichiometric. The calcite % in the dolomites oscillates around 48 to 53.3 % (Table 3.1). Also the ordering ratio of dolomites of Pazar formation ranges within 0.18 to 0.75. When the ordering ratio is plotted against the  $\text{CaCO}_3$  % scattergram (Figure 3.19), a bimodal distribution is seen in both sides of the stoichiometry field ( $\text{CaCO}_3\% = 50\%$ ) as two clusters. The more the relation diverts from stoichiometry field the more the ordering is seen in dolomites of Pazar formation.

After plotting the obtained data on the diagram of Morrow (1982), it is seen that the bimodal distribution near stoichiometry field is once more acts as an outstanding feature (Figure 3.20). The left cluster ( $\% \text{CaCO}_3 < 50$

**Table 3.1. X-ray Diffraction data of investigated dolomites.**

<b>Sample No:</b>	<b>d(104)</b>	<b>d(015)</b>	<b>d(101)</b>	<b>Order Ratio</b>	<b>% CaCO<sub>3</sub></b>	<b>% MgCO<sub>3</sub></b>
YT-1B	-	-	-	-	-	-
YT-5	-	-	-	-	-	-
YT-8	2.887	5	13	0.385	50.334	49.666
YT-9A-3	2.891	7	17	0.412	51.667	48.333
YT-10	2.891	8	14	0.571	51.667	48.333
YT-9A-10	2.884	7	13	0.538	49.334	50.666
YT-10-6	2.893	6	11	0.545	52.334	47.666
YT-8-2	2.884	7	12	0.583	49.334	50.666
YT-10-7	2.883	9	13	0.692	49.000	51.000
YT-12	-	-	-	-	-	-
YT-13-1	2.878	2	10	0.200	47.334	52.666
YT-14-2	2.89	4	13	0.308	51.334	48.666
YT-15	2.89	10	23	0.435	51.334	48.666
YT-16	2.888	11	22	0.500	50.667	49.333
YT-17	2.89	33	44	0.750	51.334	48.666
YT-17-6	2.889	6	33	0.182	51.000	49.000
YT-18-1	2.883	6	12	0.500	49.000	51.000
BK-4	-	-	-	-	-	-
BK-7	-	-	-	-	-	-
BK-7A	-	-	-	-	-	-
BK-10A	2.895	30	13	2.308	53.000	47.000
BK-11B	2.891	5	9	0.556	51.667	48.333
BK-12	2.89	4	9	0.444	51.334	48.666
BK-13	-	-	-	-	-	-
AK-2	2.896	8	17	0.471	53.334	46.666
AK-1A	2.885	5	15	0.333	49.667	50.333
AK-1C	2.893	3	7	0.429	52.334	47.666
AK-3	2.892	5	7	0.714	52.000	48.000
AK-4	2.893	6	12	0.500	52.334	47.666
AK-2D	2.888	3	8	0.375	50.667	49.333
AK-5	2.89	8	15	0.533	51.334	48.666
AK-6	-	-	-	-	-	-
AK-14	-	-	-	-	-	-

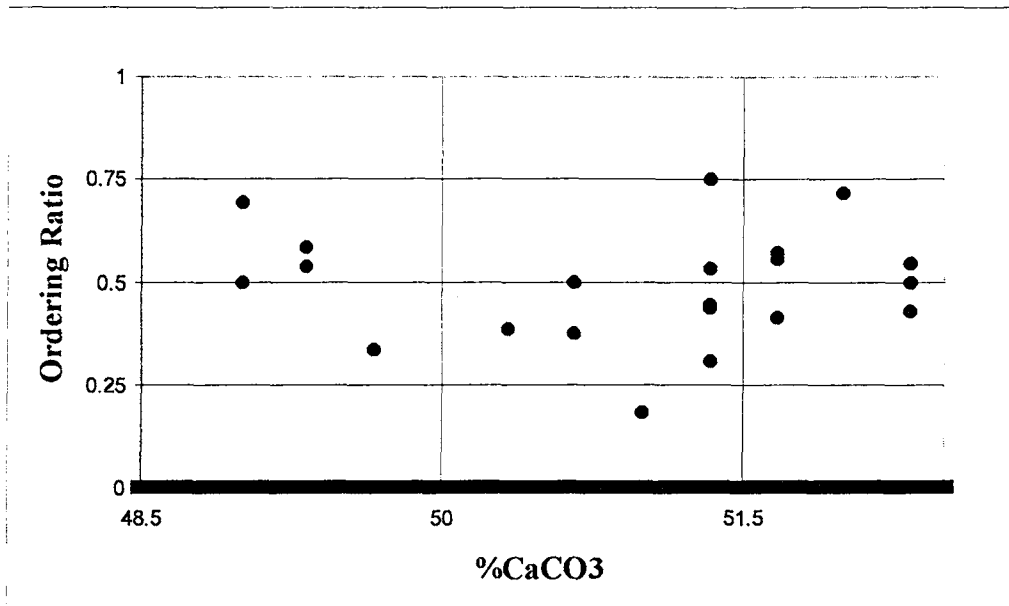


Figure 3.19.: Scattergram showing the relation of ordering ratio with %CaCO<sub>3</sub> (Hardy and Tucker, 1988).

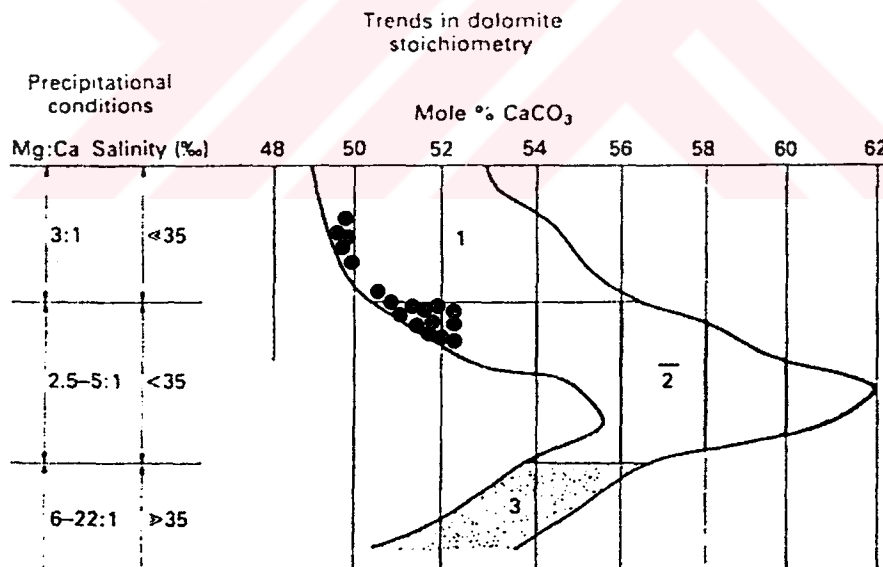


Figure 3.20.: Trends in dolomite stoichiometry data and inferred precipitational conditions. Group 1 is composed of ancient sucrosic and sparry dolomites. Group 2 is composed of finely crystalline modern and ancient dolomites not associated with evaporites and group 3 are finely crystalline modern and ancient dolomites associated with evaporites, from Morrow, 1982

%) in the Figure 3.19 falls into the “1” field, which indicates ancient sucrosic and sparry dolomites. However, the right cluster (% CaCO<sub>3</sub> > 50 %) falls into the “2” field, indicating finely crystalline modern and ancient dolomites not associated with evaporites. This relation indicates a two stage precipitational and diagenetic history of the dolomites of Pazar formation. This relation is also implicitly seen in the petrography studies as there exists two size groups and two matrix vs. rhomb relations. The smaller rhombs are seen as embedded in the clayey matrix, however the larger rhombs are seen as floating over the matrix. This second larger group is reflected by the “1” group in Figure 3.20.

### **3.2.3. Clay Mineralogy**

A total of 23 samples out of 35 randomly X-rayed samples were selected to determine the mineralogy of clay fraction of the Pazar formation. All of the selected samples are X-rayed at conditions of air dried, ethylene glycolated and heated at 300°C. After the preliminary analyses, only 7Å bearing samples were heated at 550°C. The X-ray diffraction scanning limits were defined as 2° to 30° 2θ for air dried slides, on contrary, the ethylene glycolated and heated slides were scanned from 2° to 15° 2θ, using Cu Kα. The clay minerals were identified according to Grim (1968), Carroll (1970), Pei-Yuan Chen (1977), Brindley and Brown (1980), Nemezc (1981), Wilson

(1987) and Moore and Reynolds (1989). It was observed that the constituents of clay fraction of Pazar formation were smectites, illites, chlorites and kaolinites (Figure 3.21). Smectite and illite were the dominant clay minerals whereas chlorite and kaolinite were found in minor amounts and they were hardly recognized.

Smectite group clay minerals are present in all of the studied samples in variable amounts. Smectites are easily recognized by their intensive basal reflections. It reveals that for the air dried samples the strong basal reflections range between 12 and 15 Å. When the samples are ethylene glycolated, the presence of smectite becomes evident as the peak shifts to the range of 17-18 Å. Heating the samples to 300°C and 550°C causes the expanded layers to collapse to 10Å position.

Furthermore, the  $d(060)$  peaks indicate that all of the smectites in samples of Pazar formation have 1.49-1.50 Å  $d$ -spacing values (Figure 3.22). This  $d(060)$   $d$ -spacing value range is assigned to dioctahedral smectites (Brindley and Brown, 1980; Nemezc, 1981; Wilson, 1987; Moore and Reynolds, 1989). Explicitly one sample (AK-2; Figure 3.22) exhibit peaks both at 1.49-1.50 Å range and 1.52-1.53 Å range, which can be concluded as having both di- and tri-octahedral smectites. The last word about this sample will be said after the Fourier Transform Infrared Radiation studies, later in this chapter.

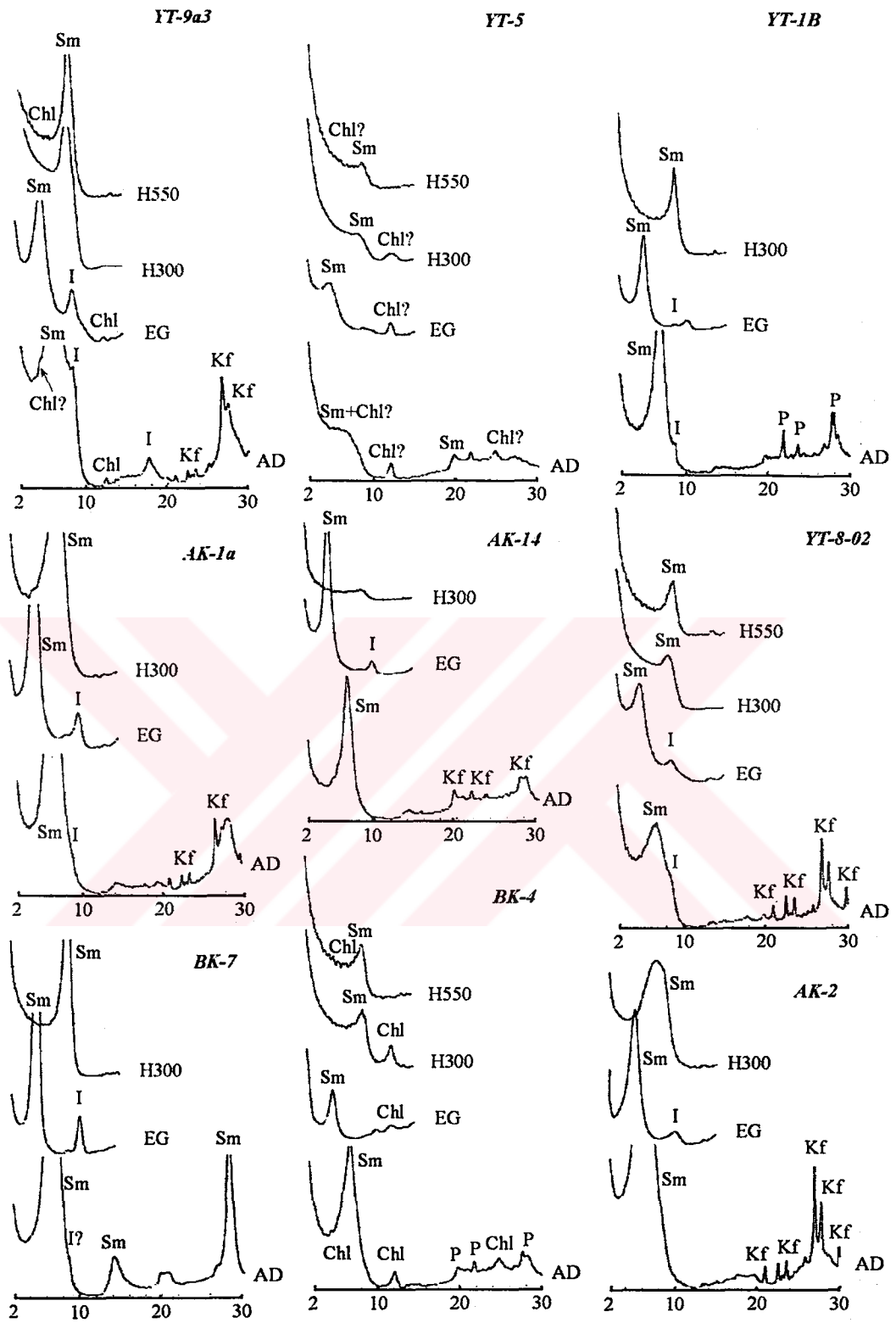


Figure 3.21.: X-ray diffraction patterns of clay fraction ( $\lt; 2\mu$ ) of Pazar formation



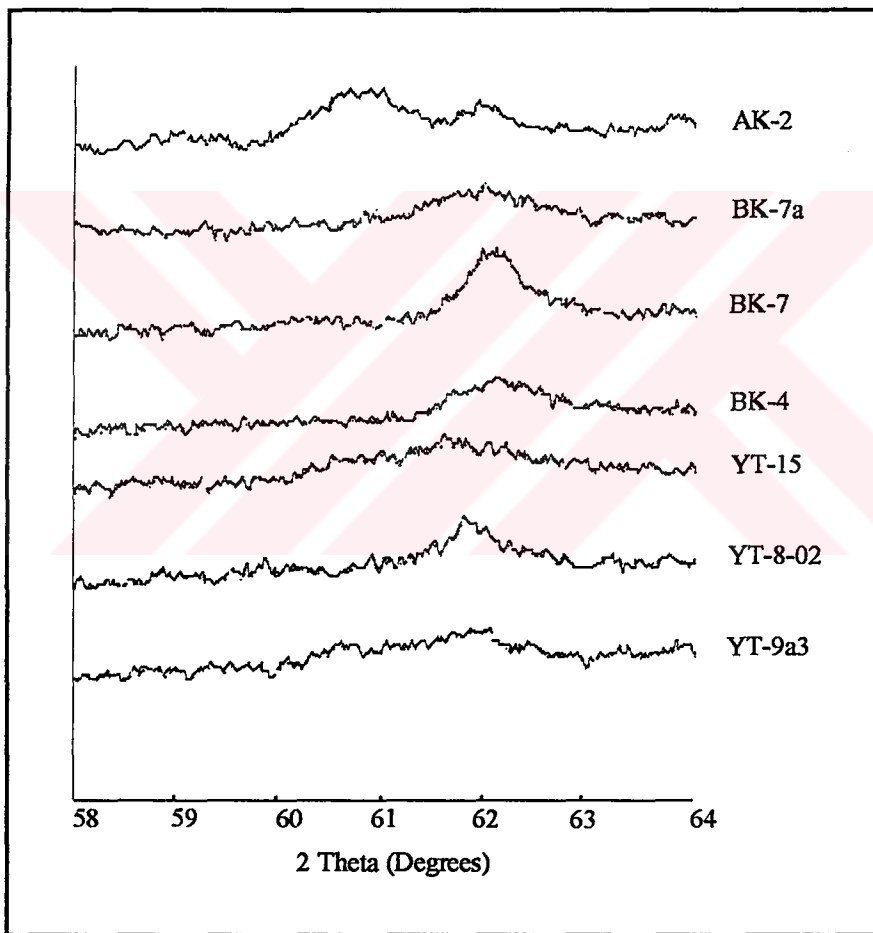


Figure 3.22.:  $\alpha$  (060) peaks of selected smectites

Likewise smectites, illites are present nearly in all of the analyzed samples. However, in some samples illite could not be detected, most probably due to the detection limits of X-ray diffraction (< 5%). The identified illites has characteristic 10Å basal reflection in all kinds of smear slides. On the other hand, only in a few samples 7 Å minerals are identified. To investigate the nature of the 7Å minerals the samples are heated at 550°C. When the semi-amorphous character of 7Å peaks are encountered after heating, these 7Å minerals are then referred as kaolinite otherwise they are cited as chlorite. Almost all of the analyzed X-ray diffraction patterns of Pazar formation show similar characteristics only 8 very representative samples are shown in Figure 3.21.

### **3.3. FOURIER TRANSFORM INFRARED RADIATION STUDIES**

Fourier Transform Infrared Radiation methods are applied to selected 8 samples after the samples are identified with respect to their purity in terms of their monomineralic clay mineralogy after X-ray diffraction studies. Extreme care was taken to select the richest sample in smectite proportion.

The Fourier Transform Infrared Radiation analyses of selected 8 smectite rich samples show considerable broadening of all the characteristic smectite IR absorption bands such as broadenings at 3630 cm<sup>-1</sup>, 920-910

$\text{cm}^{-1}$ , 890-840  $\text{cm}^{-1}$  (Figure 3.23, Table 3.2). All the samples give the OH-stretching band 3625-3630  $\text{cm}^{-1}$  and hydration (OH-stretching) bands 3405-3415  $\text{cm}^{-1}$  and 1617-1641  $\text{cm}^{-1}$  (Grim, 1968; Farmer, 1974; Jackson, 1975; Olphen and Fripat, 1979; Nemezc, 1981; Wilson, 1987 and Righi *et al.*, 1995). Samples also show variable characteristics at the  $\text{Fe}^{+3}$ ,  $\text{Al}^{+3}$  and  $\text{Mg}^{+2}$  elemental links (Table 3.2). As a consequence smectite samples have  $\text{Al}^{+3}$ ,  $\text{Fe}^{+3}$  and  $\text{Mg}^{+2}$  elements in their structures (Olphen and Fripat, 1979; Farmer, 1974; Wilson, 1987 ;Righi *et al.*, 1995). On the other hand all the samples show the similar SiO deformation and Al-O stretching bands near 650-460  $\text{cm}^{-1}$ .

According to Jackson (1975), Olphen and Fripat (1979), Nemezc (1981), Wilson (1987) and Righi *et al.* (1995), dioctahedral stretching vibrations are at 3620 to 3630  $\text{cm}^{-1}$ , so based on this, all of the smectite samples have dioctahedral structure which also supports the XRD analyses. Although the sample AK-2 gives a di- and tri-octahedral structure in X-ray diffraction studies here in Fourier Transform Infrared Radiation studies, it only exhibits a dioctahedral structure. So, it may be concluded that the trioctahedral appearance of this sample in  $\alpha$  (060) peaks can be a local effect of sample contamination or it can be only a local authigenic overgrowth.

Furthermore, the Fourier Transform Infrared Radiation spectras of the selected 8 smectite rich samples of Pazar formation were observed to be

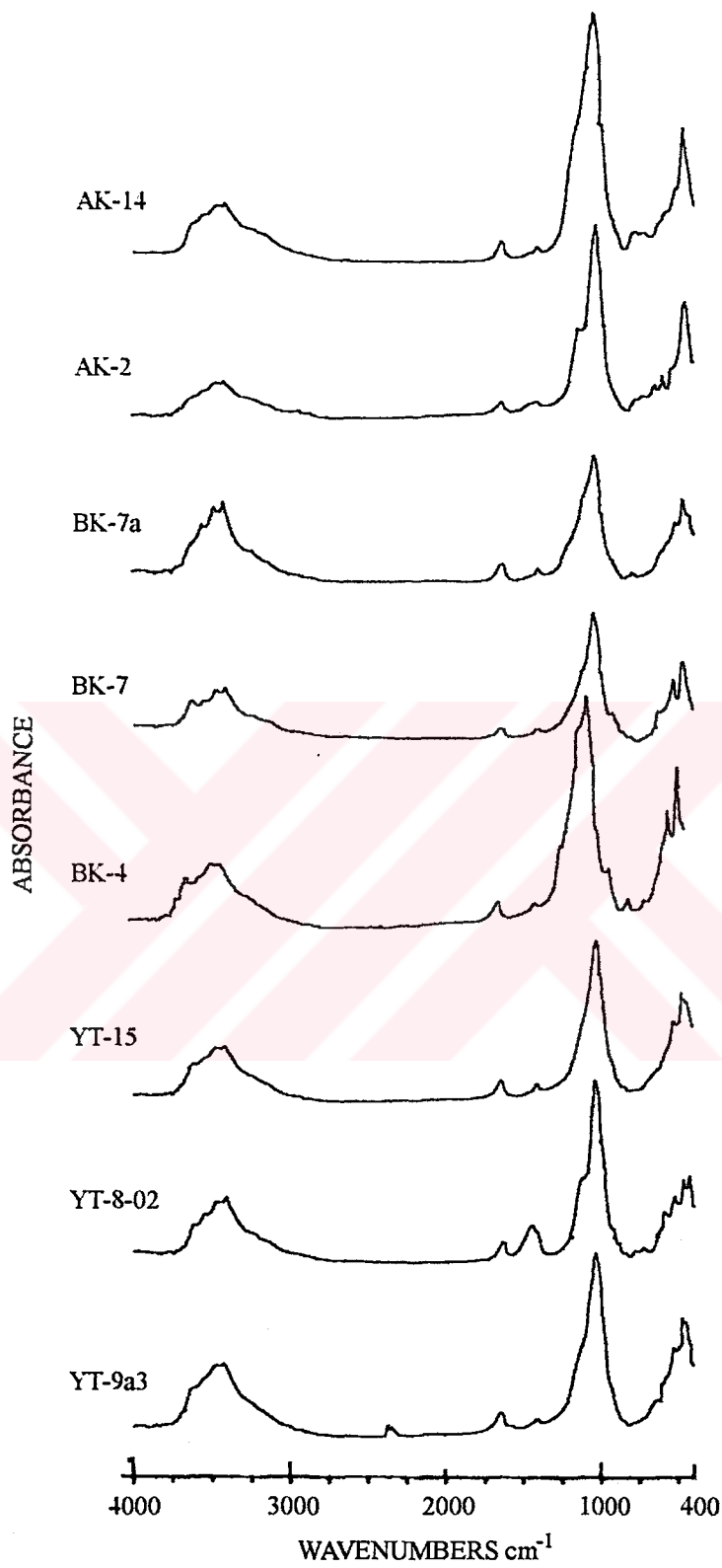


**Figure 3.23.:** Fourier Transform Infrared Radiation spectras of Pazar formation

**Table 3.2.** Fourier Transform Infrared Radiation absorptions of samples of Pazar formation, shadowed columns indicate international standard samples from Olphen and Fripat (1979).

Sample		Sample											Description
AK-14	AK-2	BK-7A	BK-7	BK-4	YT-15	YT-8-02	YT-9-A3	OECD 01	**SWy-1	***STX-1	****SAX-1		
3630	3630	3630	3630	3625	3630	3630	3630	3628	3625	3625	3616	OH- stretching	
3548	3520	3548	3548	-	-	3546	3550	-	-	-	-	-undifferentiated	
3471	-	3471	3471	3476	3490	3476	3471	-	-	-	-	-	
3415	3415	3415	3415	3415	3415	3405	3415	3425	3400	3400	3420	Hydration, OH- stretching	
1620	1620	1620	1620	1639	1641	1617	1637	1635	1625	1620	1630	Hydration, HOH deformation	
1405	1405	1400	1402	1405	1405	1435	1405	1395	1425	1400	-	carbonate	
-	1133	-	1123	1100	-	1123	-	1112	1077	1097	1095	SiO- stretching	
1046	1022	1063	1046	1046	1030	1035	1027	1037	1042	1038	1025	SiO- stretching	
-	-	920	930	905	900	915	900	918	920	918	915	OH deformation, linked to 2Al <sup>+3</sup>	
-	-	-	889	-	-	884	-	890	885	-	-	OH deformation, linked to Fe <sup>+3</sup> , Al <sup>+3</sup>	
-	-	-	840	-	838	-	838	-	850	849	840	OH deformation, linked to Mg <sup>+2</sup> , Al <sup>+3</sup>	
792	778	807	799	802	-	-	-	805	800	797	790	silica / OH deformation, linked to Mg <sup>+2</sup> , Fe <sup>+3</sup>	
-	730	-	-	700	-	730	-	795	780	-	-	silica	
-	648	-	633	-	648	-	648	627	624	630	625		
525	537	525	533	530	525	525	525	520	524	522	520	SiO Deformation and Al-O stretch	
475	470	474	475	471	475	475	475	468	468	470	465		

\*OECD 01. Dioctahedral Montmorillonite (Olphen and Fripat, 1979)

\*\* SWy-1. Dioctahedral Montmorillonite, Wyoming (Olphen and Fripat, 1979)

\*\*\* STX-1 Dioctahedral Montmorillonite, Texas (Olphen and Fripat, 1979)

\*\*\*\* SAX-1 Dioctahedral Montmorillonite, Arizona (Olphen and Fripat, 1979)

similar to that of four international standard samples, OECD 01 (dioctahedral Montmorillonite), SWy-1 (from Wyoming, dioctahedral Montmorillonite), STx-1 (from Texas, dioctahedral Montmorillonite) and SAx-1 (from Arizona, dioctahedral Montmorillonite) (Olphen and Fripat, 1979) (Table 3.2).

### 3.4. SCANNING ELECTRON MICROSCOPE STUDIES

Scanning electron microscope studies are performed to clear up the relations of previously identified non-clay and clay minerals, to arouse the micromorphology of minerals and to check the degree of alteration of the tuffs of Pazar formation. After the thin section and X-ray diffraction studies 10 samples were selected to study under Scanning Electron Microscope. The samples were coated with Gold-Palladium (Au-Pd) alloy to overcome the non-conducting phenomenon of the minerals (Sudo *et al.*, 1981 and Wilson, 1987).

The siliceous shell bearing organisms (Diatomacea?) exhibit lenticular forms which are rectangular in cross section (Figure 3.24). They have lenticular relatively smaller slits on their walls and they appear to have covering limbs. (Sample No: YT-4, Figure 3.25).

The dolomites of Pazar formation show perfect euhedral rhombohedral crystal outlines which are seen in Figure 3.26 (Sample No: YT-10-03). The sizes of these dolomites vary from 1 to 6  $\mu\text{m}$ , which also

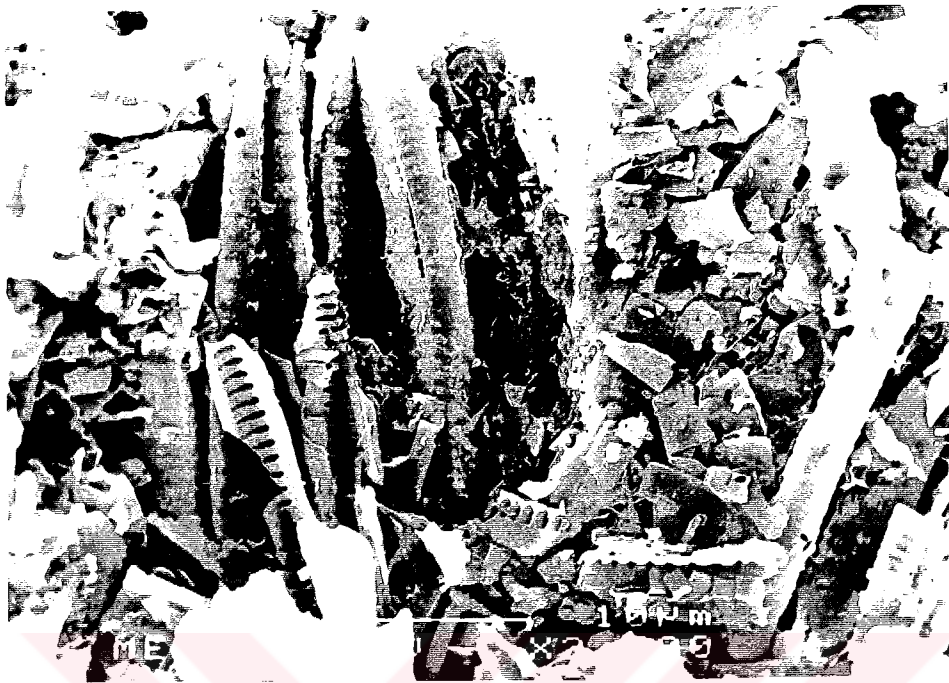
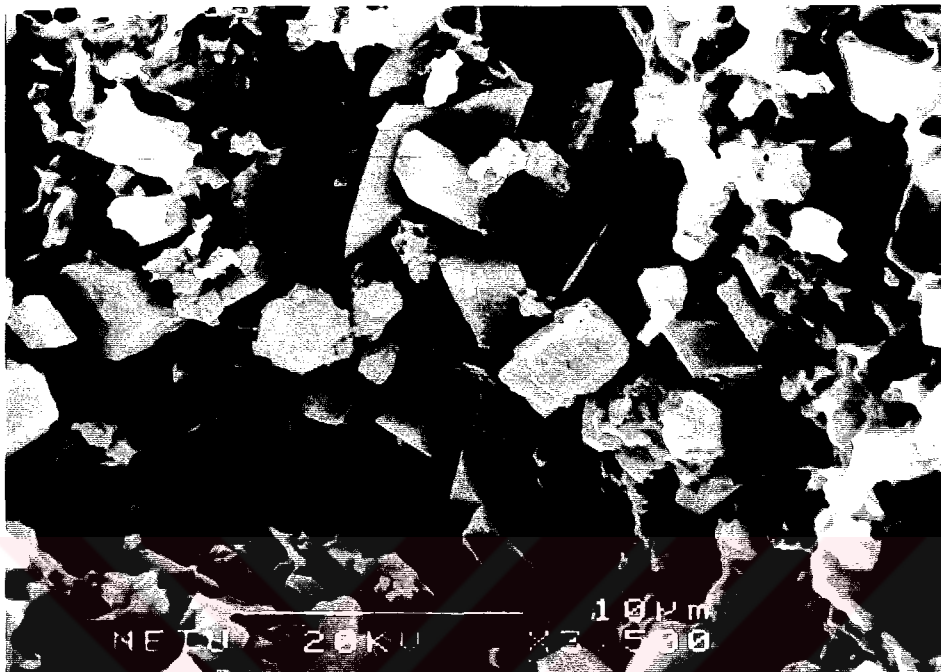


**Figure 3.24.:** Scanning electron micrograph showing lenticular structure of Diatomacea (?), X2000, Sample No: YT-4



**Figure 3.25.:** Scanning electron micrograph showing the limbs and slits of Diatomacea (?), X3500, Sample No: YT-4



DEPT. OF METALLURGICAL ENG. METU/ANFARA WED 27-MAR-96 14:57  
 Cursor: 0.000keV = 0

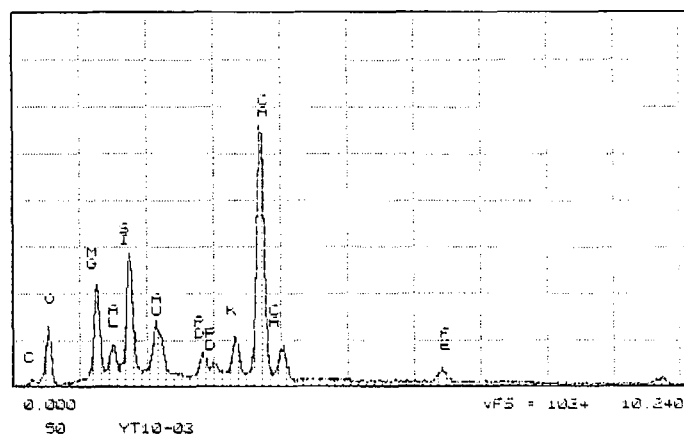


**Figure 3.26.:** Scanning electron micrograph showing dolomite rhombs and its EDX, X3500, Sample No: YT-10-03



support the petrographic name dolomicrite given through the petrography studies. Moreover, the EDX analysis of this sample reveals the presence of Ca, Si, Mg, O and minor amount of K and Fe. The low amount of C is not an abnormal situation as the Au-Pd alloy coat absorbs the C reflectance. The K-feldspars of Pazar formation is suspected to be authigenic in the studied samples since they show well grown euhedral crystal outlines (Sample No: BK-7, Figures 3.27 and 3.28). In addition the EDX of K-feldspars in sample AK-6 (Figure 3.28) point out the presence of Si, Al, Mg, K, Ca and O.



**Figure 3.27.:** Scanning electron micrograph showing authigenic K-feldspar crystals, X2000, Sample No: BK-7.

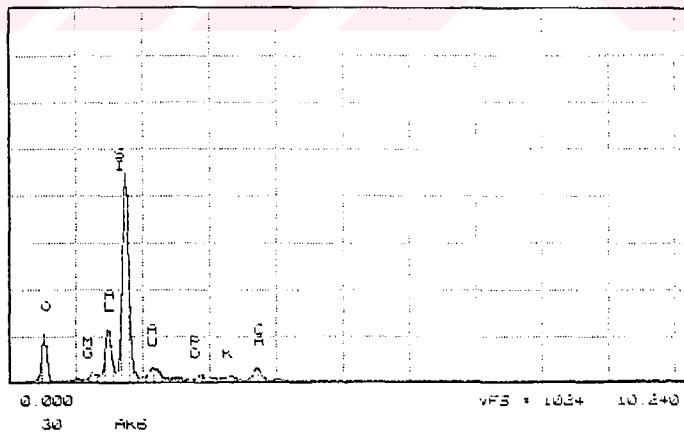


**Figure 3.28.:** Scanning electron micrograph showing authigenic K-feldspars in analcime rich mudstone and its EDX, X2000, Sample No: AK-6.

Although only analcime is mentioned as zeolite in the X-ray diffraction studies; scanning electron microscope studies show that there exists some other kinds of fibrous zeolites. The analcime crystals do not have perfect euhedral crystal outline (Figure 3.29) but the other zeolite (erionite ? or mordenite ?) has a well developed fibrous and scattered habit grown on a silicified wood particle (Figure 3.30). The analcime sample prevails the elements Si, Al, Na and O under EDX analysis (Figure 3.29).

The pumice particles and vitric shards of tuffs of the Pazar formation generally exhibit very slightly altered states (Figures 3.31, 3.32 and 3.34). Also the EDX analysis on the vitric shard indicate the presence of Si, O, Ca and K (Figure 3.34). Furthermore, in detail some authigenic clay minerals (smectites) are seen as growing over and around the pumice fragments (Figure 3.33). On the contrary some of the tuff samples are moderately weathered, yielding to grow clay minerals authigenically in their void interparticle spaces, which alter the pumice rich part of the tuff layer (Figure 3.35).

In general in the scanning electron microscope study of samples of Pazar formation, the most common mineral was the smectite, present almost in every scene. The typical view of the honey comb structure of smectite is seen in Figure 3.36.

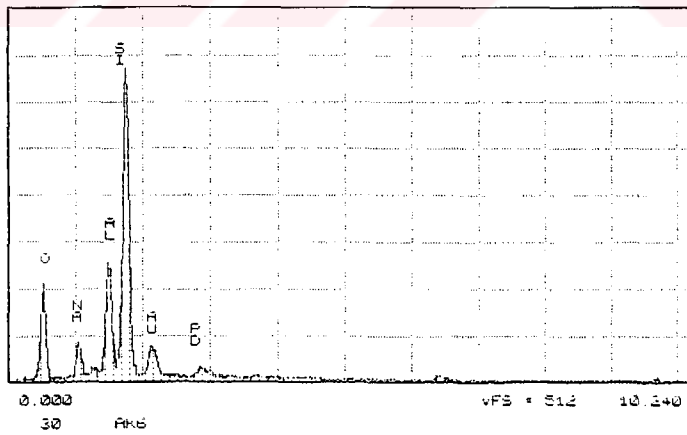
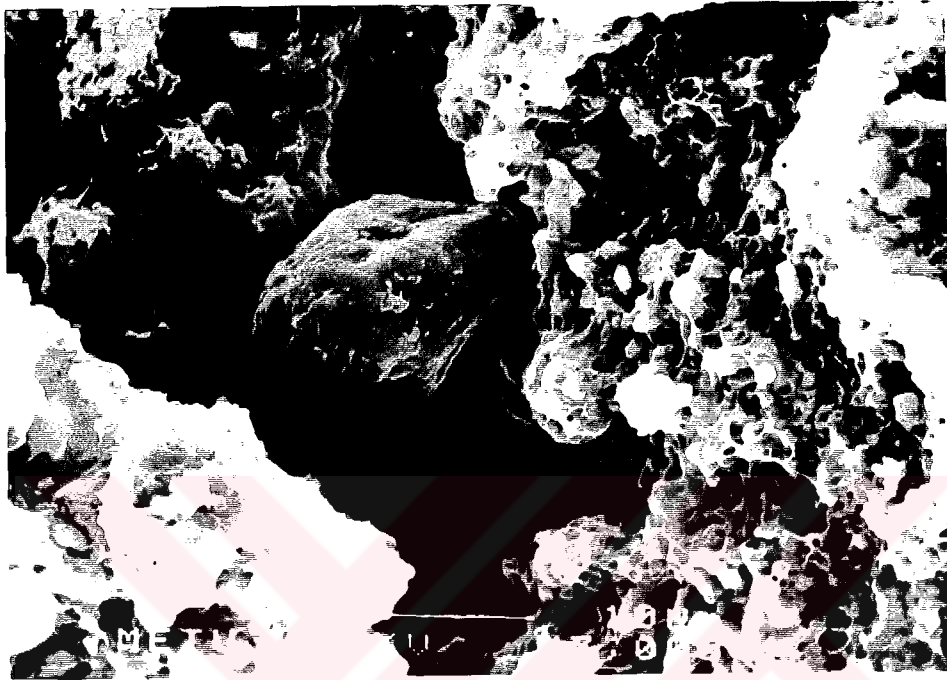


**Figure 3.29.:** Scanning electron micrograph showing analcime crystals and its EDX, X3000, Sample No: AK-6.



**Figure 3.30.:** Scanning electron micrograph showing fibrous zeolites (Erionite ? or mordenite ?) on silicified wood, X 1000, Sample No: BK-7.



**Figure 3.31.:** Scanning electron micrograph showing internal structure of pumice particles, X1000, Sample No: YT-12.



**Figure 3.32.:** Scanning electron micrograph showing a well preserved glass shard, X 1000, Sample No: AK-8A.



**Figure 3.33.:** Scanning electron micrograph showing the close up view of relations between a pumice fragment and authigenically grown smectites, X1500, Sample No: AK-14.

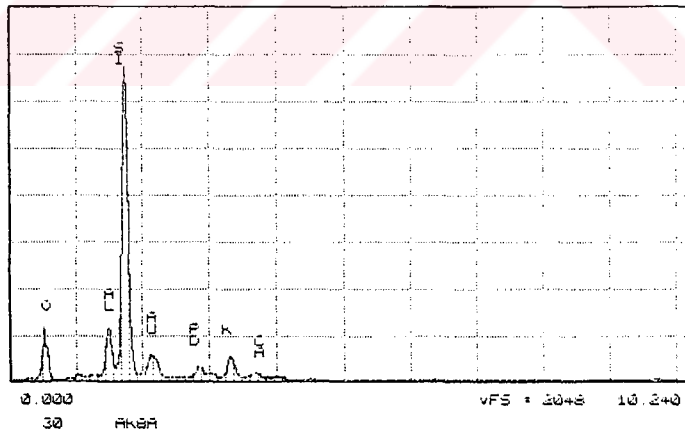


**Figure 3.34.:** Scanning electron micrograph showing a glass shard and its EDX, X1000, Sample No: AK-8A.

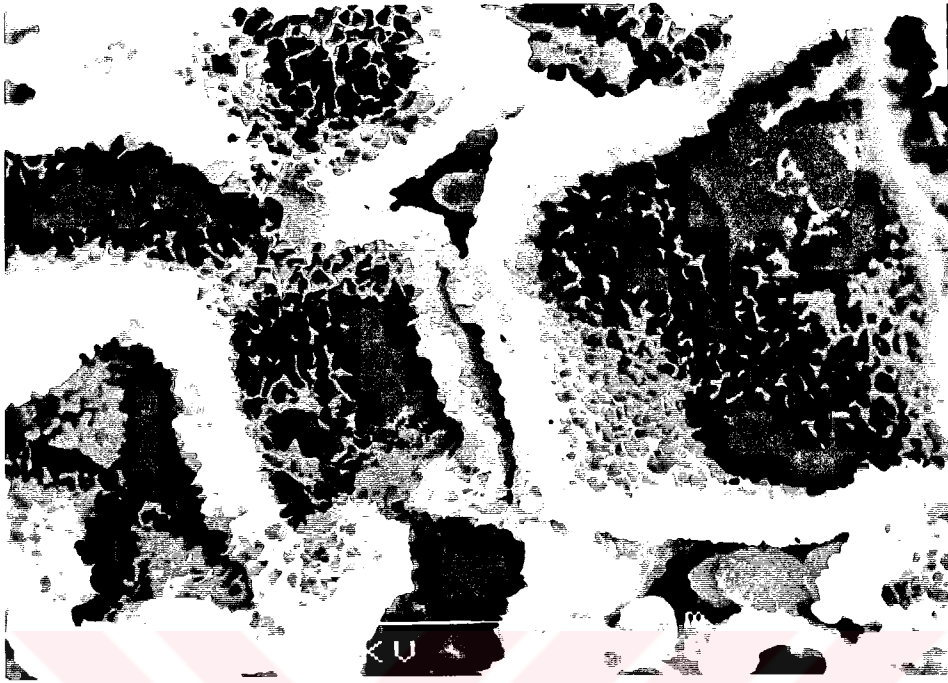


**Figure 3.35.:** Scanning electron micrograph showing authigenic smectites grown in the pore spaces of pumices, X 2000, Sample No: YT-4.

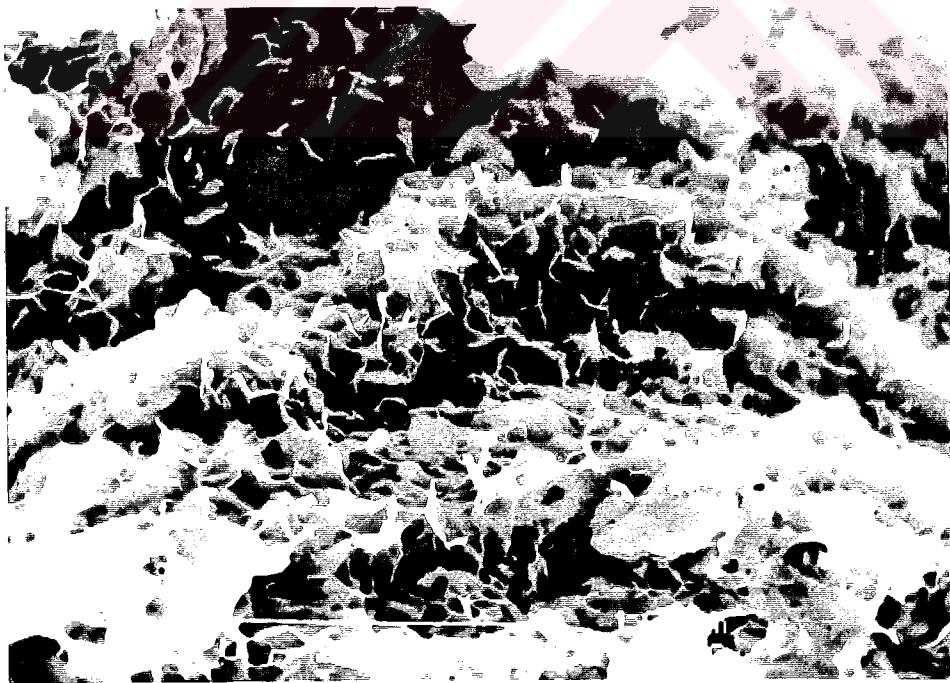


**Figure 3.36.:** Scanning electron micrograph showing the typical honeycomb structure of smectites, X 3700, Sample No: AK-14.



## CHAPTER 4

### DISCUSSION OF RESULTS

#### 4.1. GEOLOGY:

The results of field and remote sensing studies show that the basin has an ellipsoidal shape covered with Galatean volcanics at every directions (Figures 2.1 and 2.2). The Digital Elevation Model, field and remote sensing studies also show that the basin fill deposits show a low land topography whereas the Galatean volcanics exhibit a highland topography (Figures 2.3, 2.4 and 2.5). The sources of these volcanics are five known eruptive centers distributed around the basin (Tankut *et al.*, 1995). Only in the south, the Bayındır fault forms a barrier that bounds the basin. However, the outcrops of the Pazar formation are also observed in further south of the Bayındır fault (Figures 2.1 and 2.2). This suggests that the age of the faulting is slightly later than the depositional history of the basin. Furthermore, the stratigraphic relations of Pazar formation with Galatean volcanics suggest that their age should be the same. In the type area, the age of the Pazar formation extends through Early Pliocene (?) with breaks, based on the

presence of vertebrate fossils. Thus, the age of the whole system can be assigned as Early Miocene-Early Pliocene (?).

In the Landsat 5 TM scenes the Pelitcik basin seem to have a connection with the Çeltikçi Graben in the south before the faults have started to develop. On the other hand, using Landsat 5 TM scenes, three pilot areas are selected from the most uncovered/unvegetated areas of the Pazar formation. Also numbers of volcanoclastic lenses are mapped in the study area by using the multispectral character of Landsat 5 TM scenery. The volcanoclastic lenses are generally elongated mostly in the NE-SW and E-W directions. They are believed to be fed from northwest and north of the basin (Toprak, 1996, personal communication). There are three clues for this argument 1) their direction of elongation is parallel to the bedding direction and perpendicular to the feeding direction (NE-SW and E-W), 2) all of the volcanoclastic lenses pinch out towards south, 3) no volcanoclastic lenses are observed in the southern parts of the basin. On the other hand, presence of crossbeddings in the volcanoclastics show that there exists a high energy fluvial environment near to the shores of the lake, in the spasmodic activities of volcanism and/or tectonism. The same situation is also valid for the generation of volcanoclastic lenses in the basin.

Even though volcanics are kept beyond the scope of this thesis, a zone of Multiple-Rim Accretionary Lapilli rich tuff is encountered as embedded in the volcanoclastics near Yoncatepe village. Although the single

appearance of this tuff type has no contribution to the paleoenvironmental discussion, it preserves very valuable information to the volcanology of this area. A detailed volcanological study, will yield parameters about the nature, type and internal structure of this eruption, in which these parameters can be extrapolated to the eruption center. Also, a detailed sedimentological study of these tuffs will give the location of the eruption center.

The generalized stratigraphic section of the Pazar formation reveal gray to green claystones/mudstones, white dolomicrites, tuff layers, thin coal beds and white cherty limestones (Figure 2.7).

Subsequently the green color of mudstones and claystones indicate a perennial lake that scarcely dries up and generally fed by fresh water (Hubert *et al.*, 1976; Smith *et al.*, 1983). The thin bedded character, lack of continuous thickness of shales or carbonates and repetitive stratigraphy (Figures 2.11, 2.13 and 2.16) suggest deposition in relatively shallow water (Yuretich *et al.*, 1984) The stratigraphic location and presence of coal beds, organic rich shales and silicified woods, especially in Yoncatepe and Buğralar sections, indicate that these outcrops represent the shore facies of a lake which have shallow character. The deepest facies of this lake is represented by Ostracoda and Pelecypoda rich limestones in the Akkayatepe section, in the southern parts of the basin. In addition, the strike and dip measurements indicate that the deepest facies of this shallow lake is submerged by the Çamlıdere Reservoir. Moreover, the presence of cherty

limestones in Yoncatepe and Buğralar sections reveals water level fluctuations in the evolutionary history of the lake.

Presence of the volcanic complexes serves not only as the detrital source for the lake, but tuff eruptions from the volcanic centers also serve as the source for silica for the lake. This phenomenon is reflected by the flourishing of diatom frustules (?), vitric tuffs, silicified woods and chert layers in the measured sections also support this fact. On the other hand, the absence of oolitic sediments indicate a quiet lacustrine environment.

#### **4.2. MINERALOGY:**

The petrographic, X-ray diffraction, scanning electron microscope and Fourier Transform Infrared Spectroscopy studies reveal that the major non-clay minerals of the Pazar formation are dolomite, K-feldspar and plagioclase (Figures 3.15, 3.16 and 3.17). Furthermore, as a non-clay mineral and as a zeolite, analcime is found both in X-ray diffraction and scanning electron microscope studies in the samples of Akkayatepe section (Sample No: Ak-5, Ak-6; Figures 3.17 and 3.29). Trace amounts of erionite (?) is identified only during the scanning electron microscope studies in the silicified wood samples of Buğralar sequence (Sample No: BK-7, Figure 3.30). Although saline minerals such as trona are not encountered in the Pazar formation, only very minor gypsum veins are present throughout the whole sequence. The clay minerals of the Pazar formation have an acute

variation in their types. The dominant clay mineral is smectite, whereas illite has a minor contribution, but chlorite and kaolinite are in trace amounts in the clay mineralogy of the Pazar formation (Figure 3.21).

Although pumice fragments and glass shards are seen as fresh in the petrography studies (Figures 3.3, 3.4 and 3.12), the bubble-wall shards are seen as fresh and/or slightly altered to smectite in scanning electron microscope studies (Figures 3.31, 3.32, 3.33, 3.34 and 3.35). In addition, fresh diatom frustules (?) are also found. This unaltered to slightly altered state of diatoms, pumices and shards indicate that the lake waters that are trapped in the tuffs were not saline enough and the pH of the water was not alkaline enough to alter them (Sheppard, 1989)

In almost all of the samples, minerals of various K-feldspars exist. In tuffaceous and analcime rich samples they are seen as authigenically grown in the pore spaces (Figures 3.27 and 3.28). However, in the non-tuffaceous lithologies they are believed to have a detrital origin, as the authigenic formation of K-feldspars in a volcanic lacustrine environment requires a zeolitic precursor in their paragenetic sequences (Sheppard and Gude, 1968; Mariner and Surdam, 1970; Surdam and Parker, 1972; Surdam and Sheppard, 1978; Hay, 1978; Boles and Surdam, 1979; Jones and Weir, 1983; Hay and Guldman, 1987; Remy and Ferrell, 1989; Sheppard and Fitzpatrick, 1989; Sheppard, 1989, 1991, 1994; Stamatakis, 1989 a, b; Altaner and Grim, 1990; de Pablo-Galan, 1990; Banfield *et al.*, 1991).

Dolomite is encountered nearly at almost all of the samples. Furthermore, not only its presence but its' indications about the water chemistry should have to be mentioned. The dolomite rich lithologies are petrographically named as dolomicrite, according to the size of rhombs (Morrow, 1982). Two size groups of rhombs are present in the thin sections; i) rhombs smaller than  $6\mu\text{m}$  and ii) rhombs grater than  $8\mu\text{m}$  but smaller than  $10\text{-}15\ \mu\text{m}$ . The greater rhombs resemble to float over the associated matrix. This habit indicates a latter diagenetic history.

There have been vast researches in the formation mechanism of dolomites and it is found that dolomites are resulted from evaporative pumping, burial diagenesis, fresh and mixing water impacts, dilution of water, pressure and sabkha evaporation (Adams and Rhodes, 1960; Picard and High, 1972; Badiozamani, 1973; Folk, 1974; Wolfbauer and Surdam, 1974; Folk and Land, 1975; Surdam and Wolfbauer, 1975; Hubert *et al.*, 1976; Desborough, 1978; Boles and Surdam, 1979; Friedman, 1980; McKenzie *et al.*, 1980; Muir *et al.*, 1980, 1982; Yuretich and Cerling, 1983; Remy and Ferrell, 1989; Warren, 1991). Most of these models require evaporation or burial as triggering mechanisms and consider dolomite formation as a secondary diagenetic event. In contrast there exists some primary poorly ordered non stoichiometric dolomites in nature (Lumsden and Chimausky, 1980; Morrow, 1978; Morrow, 1982). The Mg/Ca ratio and salinity are found to be the pre-eminent controls over dolomite

crystallization (Goldsmith and Graf, 1958 b; Berner, 1971; Folk, 1974; Folk and Land, 1975; Morrow, 1978; Lumsden and Chimausky, 1980; Morrow, 1982, Yuretich and Cerling, 1983). So the stoichiometry and ordering ratios are the most striking features in determining the primary state of dolomite mineral.

As noted above there are two clusters based on size, unsurprisingly the chemistry and ordering of dolomites also indicate such a dual distribution. There exists two clusters in the % CaCO<sub>3</sub> vs. ordering scattergram, in which the larger (ii) group represents the calcium depleted cluster (Figure 3.19). Furthermore, when the mole % CaCO<sub>3</sub> are plotted in the Figure 3.20, it is seen that the larger rhombs fall into the "1<sup>st</sup>" group, in which the salinity is ≤35 ‰ and Mg/Ca ratio is  $\frac{3}{1}$ . Whereas in the smaller ones the salinity is < 35 ‰ and Mg/Ca is  $\frac{2.5-5}{1}$  (Figure 3.20). These poorly to moderately ordered dolomites indicate a fresh environment rich in Mg<sup>+2</sup>. On the time of dolomite forming side, the finely grained (cluster 2) indicates a primary deposition or syndepositional (penecontemporaneous) to pre-burial replacement due to its conformable mass with the other lithologies, fine size, non-stoichiometric character and non-associated state with evaporite (saline) minerals (Goldsmith and Graf, 1958 b; Lumsden and Chimausky, 1980; Morrow, 1982; Yuretich *et al.*, 1984). However, the other group (cluster 1) indicate a post depositional diagenetic phase. Also the

presence of dolomite in such an environment indicates that the pH of the lake waters should be less than 8.5-8 and the activity of  $H^+$  is buffered by dolomite (Surdam and Parker, 1972).

Although analcime is reported only in two samples (Figure 3.17) as a zeolite, it reveals important chemical clues for water chemistry. Two basic parameters are highly required for the formation of analcime; 1) presence of  $Na^+$  or high  $\frac{Na^+}{H^+}$  activities, and 2) a basic environment in which pH is greater than 7 (Picard and High, 1972). The absence of analcime in the remainder of the section can be explained as the  $Na^+$  depletion relative to other cations at these times. The increase of  $Na^+$  in a lake environment is an indication of increasing salinity (Dyni, 1976; Yuretich and Cerling, 1983).

The dominant clay mineral in the lacustrine facies of the Pazar formation is found to be smectite. The remaining clay minerals are illites in minor, chlorite and kaolinites in trace amounts that can hardly be identified. The structure of smectites are found to be Al-Fe dioctahedral (Figure 3.22, 3.23) in which they indicate detritic in origin, that come through the high lands of Galatean Volcanic Province. Authigenic smectites are only found in the tuffaceous lithologies of the Pazar formation, especially in the pore spaces of pumices and as overgrowths on the pumice fragments (Figure 3.35). Also formation of authigenic smectite increases pH, increasing pH yields as more dissolution of volcanic glass (Jones and Weir, 1983), but on the other hand presence of dolomite makes a barrier for the increase of pH



as it buffers the  $H^+$  activity. In addition  $Mg^{+2}$  ions are trapped by dolomite in the solution, which also slows down the crystallization rate of  $Mg^{+2}$  rich smectite (Dyini, 1976; Yuretich and Cerling, 1983).

Based on all the above facts the Neogene Pelitçik lake can be inferred as perennial, shallow, quiet lacustrine environment having fresh to slightly saline  $\leq 35$  ‰ and alkaline  $7 < pH < 8.5$  water chemistry. Also the Mg/Ca ratio should be less than  $\frac{2.5-5}{1}$ .

The geographic situation, mineral assemblage and water chemistry indicate that the lake has started its evolution as a hydrologically open lake that has an outlet in the south (Hay and Sheppard, 1977; Allen and Collinson, 1986). The activation of Bayındır fault and/or Çeltikçi fault must have been simulated in the lake as phase change from open lake state to closed state, and reflected in the mineralogy as an increase in  $Na^+$ ; accordingly increase in salinity and formation of analcime. This is also supported by the presence of tiny gypsum veins in the non-carbonate lithologies of Akkayatepe section.

The total thickness of the Pazar formation is 610 meters, and nearly two third of it is composed of claystones and dolomicrites. Furthermore approximately 80% of the clay fraction of these claystones are composed of smectites. This smectite accumulation can be utilized for industrial usage, after industrial quality control and quality assurance tests are performed.

## CHAPTER 5

### CONCLUSIONS

The additional arguments to the existing literature, obtained from geological and mineralogical investigations of Pelitçik Neogene lacustrine basin can be summarized as follows:

1. Various volcanoclastic lenses are mapped in the study area and their feeding direction is found to be northwest and north relative to the basin.

2. Nine tuff layers of the Pazar formation are identified and named petrographically. Multiple rim accretionary lapilli tuff was identified for the first time in the vicinity of the study area.

3. The non-clay mineralogy of Pazar formation is determined by means of petrography, X-ray diffraction and scanning electron microscope studies, and it is composed of K-feldspar, dolomite, minor plagioclase and quartz.

4. The presence of zeolite (Analcime and erionite ?) was identified for the first time in the study area.

5. K-feldspars in the tuffaceous rocks were found to be authigenic in their pore spaces.

6. Dolomites in the study area are classified according to their stoichiometric character. Two clusters have been found: i) large rhombs of diagenetic origin, ii) finer rhombs of syndepositional or early diagenetic origin.

7. No saline or evaporite group minerals were found in the study area except very tiny gypsum veins.

8. Clay mineralogy of the Pazar formation is determined by means of petrography, X-ray diffraction, Scanning Electron Microscope and Fourier Transform Infrared Radiation studies. The dominant clay mineral is dioctahedral Fe-Al rich smectite, indicating a detritic origin. Authigenic smectite is confined only to the pores of pumice fragments and shards. The other clay minerals were found as illite (minor), chlorite and kaolinite (trace).

9. The presence of siliceous shell bearing organisms (Diatomacea ?) was reported for the first time in this region.

10. Lake is inferred as perennial, shallow and quiet lacustrine environment with a water chemistry of fresh to slightly saline and slightly alkaline. The Mg/Ca ratio of the lake should be less than  $\frac{2.5-5}{1}$ .

11. The lake was hydrologically open having an outlet in south in its early stages, but the activation of Bayındır and/or Çeltikçi fault turns the lake into a hydrologically closed system in its mature stages.

12. Significant amounts of smectite deposits are encountered in the Pelitçik Neogene Lacustrine basin.

**Suggestions for further studies:**

A detailed volcanological study must be carried out in coordination with geophysical methods (Gravity and Airborne Magnetic), in order to determine the structure, distribution and locations of main and parasitic eruptive centers. The afore mentioned economically feasible smectite rich layers and tuff layers should be tested for the needs of various sectors of the industry.

## REFERENCES

- Adams, J.E. and Rhodes, M.L., 1960, Dolomitization by Seepage Refluxation, Bull.Amer.Assoc.Pet.Geol., V.44, 1912-1920.
- Akyol, E., 1969, Ankara-Kızılcahamam, Çeltikçi Civarında Bulunan Kömür Zuhurlarının 1/25.000 Ölçekli Detay Jeolojik Etüdü Hakkında Rapor, MTA, Report. No: 4405 (Unpublished-Yayımlanmamış)
- Allen, P.A. and Collinson, J.D., 1986, Lakes, in H.G.Reading, Sedimentary Environments And Facies, Blackwell Sci.Pup Co., Oxford, 63-94.
- Altaner, S.P. and Grim, R.E., 1990, Mineralogy, Chemistry, and Diagenesis of Tuffs in the Sucker Creek Formation (Miocene), Eastern Oregon, Clays and Clay Minerals, 38, 561-572.
- Badiozamani, K., 1973, the Dorag Dolomitization Model -Application to the Middle Ordovician of Wisconsin, Jour. Sed.Petrology, V.43, 965-984.
- Banfield, J.F.; Jones, B.F. and Veblen, D.R., 1991, An AEM-TEM Study of Weathering and Diagenesis, Abert Lake, Oregon: I.Weathering Reactions in the Volcanics, Geochimica Et Cosmochimica Acta, 55, 2781-2793.
- Bender, F., 1955, Kızılcahamam-Ayaş Arasındaki Bölgede Petrol İhtimalleri Hakkında Rapor. MTA Report No: 2303, (Unpublished-Yayımlanmamış)
- Berner, R.A., 1971, Principles of Chemical Sedimentology, Mcgraw Hill Co., Newyork, P.240.
- Boles, J.R. and Surdam, R.C., 1979, Diagenesis of Volcanogenic Sediments in a Tertiary Saline Lake: Wagon Bed Formation, Wyoming., Amer.J.Sci., 279, 832-853.
- Brindley, G.W. and Brown, G., 1980, Crystal Structures of Clay Minerals and their X-Ray Identification, Mineral. Soc., London, 595 P.

- Carroll, D., 1970, Clay minerals A Guide to their X-Ray Identification. Geol. Soc. of Amer. Spec.Pap, No: 126, 80 P.
- Chamley, H., 1989, Clay Sedimentology, Springer-Verlag, New York, 673 P.
- Çopur, M., 1972, Ankara İli Kil İmkanlarının Genel Jeolojik Ve Ekonomik Prospeksiyon Raporu, MTA Report No: 4914, (Unpublished-Yayımlanmamış)
- De Pablo-Galan, L., 1990, Diagenesis of Oligo-Miocene Vitric Tuffs to Montmorillonite and K-Feldspar Deposits, Durango, Mexico, Clays and Clay Minerals, V.38, 426-436.
- Degens E.T., Von Herzen R.P. and Wong H.K., 1971, Lake Tanganyika: Water Chemistry, Sediments, Geological Structure, Naturwissenschaften, 59, 229-241.
- Desborough, G.A., 1978, A Biogenic-Chemical Stratified Lake Model For the Origin of Oil Shale of the Green River Formation: An Alternative to the Playa Lake Model, Geol.Soc.Amer.Bull., V.89, 961-971.
- Dyni, J.R., 1976, Trioctahedral Smectite in the Green River Formation, Duchesne County, Utah, USGS, Prof.Pap. 967, P.14.
- Erol, O., 1955, Koroğlu-Işık Dağları Volkanik Kütlesinin Orta Bölümleri İle Beypazarı-Ayaş Arasındaki Neojen Havzasının Jeolojisi Hakkında Rapor, MTA Report No: 2279, (Unpublished-Yayımlanmamış).
- Farmer, V.C., 1974, the Infrared Spectra of Minerals, Mineralogical Society Monograph 4, Allard and Son Ltd., London, 539 P.
- Fisher, R.V., and Schminke, H.U., 1984, Pyroclastic Rocks. Springer-Verlag, Berlin, P.472.
- Folk, R.L., 1974, the Natural History of Crystalline Calcium Carbonate: Effect of Magnesium Content and Salinity, Jour. Sed. Petrology, V.44, 40-53.
- Folk, R.L. and Land, L.S., 1975, Mg/Ca Ratio and Salinity: Two Controls Over Crystallization of Dolomite, Amer.Assoc.Pet.Geol., V.59, 60-68.
- Friedman, G.M., 1980, Dolomite is an Evaporite Mineral: Evidence from the Rock Record and from Sea-Marginal Ponds of the Red Sea, in D.H. Zenger, J.B.Durham and R.L. Ethington, eds. Concepts and Models of Dolomitization: Soc. Econ. Paleontol. Minerals. Spec. Publ. 28, 69-80.
- Geologic Map of Turkey, 1961-1964, 1:500.000, MTA, Ankara.

- Goldsmith, J.R. and Graf, D.L., 1958 a, Relation Between Lattice Constants and Composition of Ca-Mg Carbonates: Amer.Miner., V43, P84-101.
- Goldsmith, J.R. and Graf, D.L., 1958 b, Structural and Compositional Variations in Some Natural Dolomites, Jour. Geology, V.66, 678-693.
- Grim, R.E., 1968, Clay Mineralogy, Mc.Graw Hill, New York, 596 P.
- Hardy, R. and Tucker M., 1988, X-ray Powder Diffraction of Sediments, in Techniques in Sedimentology, M. Tucker, Ed., Blackwell Scientific Publications Co., Oxford, 191-228.
- Hay, R.L., 1966, Zeolites and Zeolites Reactions in Sedimentary Rocks, Geol.Soc.Amer.Sp.Pap.,85, P.130.
- Hay, R.L., 1978, Geologic Occurrence of Zeolites, in Natural Zeolites: Occurrence, Properties, Use, L.B. Sand and F.A., Mumpton, Eds., Pergamon Press, Elmsford, New York, 145-175.
- Hay, R.L. and Guldman, S.G., 1987, Diagenetic Alteration of Silicic Ash in Searles Lake , California, Clays and Clay Minerals, 35, 449-457.
- Hay, R.L. and Sheppard R.A., 1977, Zeolite in Open Hydrologic Systems: in Mineralogy and Geology of Natural Zeolites, F.A. Mumpton, Ed., Reviews in Mineralogy, 4, Mineral.Soc.Amer., Washington, D.C., 93-102.
- Hubert, J.F., Reed, A.A. and Carey, P.J., 1976, Paleogeography of the East Berlin Formation, Newark Group, Connecticut Valley, Amer.Jour. Sci., V 276, 1183-1207.
- İrkeç, T. and Gençoğlu, H., 1993, Kıbrısık Area (Bolu Province, North-Central Turkey)in Utilization of Sepiolitic and Mg Bearing Clays in Turkey, ITIT Report of Project 90-1-5, 177-227.
- Jackson, M.L., 1975, Soil Chemical Analysis: Advanced Course, Madison, Wisconsin Pub., USA.
- Jones, B.F. and Weir, A.H., 1983, Clay Minerals of Lake Abert, An Alkaline, Saline Lake, Clays and Clay Minerals, 31, 161-172.
- Kalafatçioğlu, A. and Uysallı, H., 1964, Beypazarı - Nallıhan - Seben Dolayının Jeolojisi, MTA Bull., 62, 1-10.
- Keller, J., Jung, D., Eckhardt, F.- J. and Kreuzer, H., 1992, Radiometric Ages and Chemical Characterization of the Galatean andesite Massif, Pontus, Turkey. Acta Vulcanologica, Marinelli Volume, 2, 267-276.

- Kerr, P.F., 1977, *Optical Mineralogy*, Mcgraw Hill, New York, 492 P.
- Ketin, İ., 1966, Anadolu'nun Tektonik Birlikleri, MTA Bull. V.66.
- Ketin, İ., 1977, Türkiye'nin Başlıca Orojenik Olayları ve Paleocoğrafik Evrimi: MTA Bull. V.88, 1-4.
- Khury, H.N. and Eberl, D.D., 1979, Bubble Wall Shards Altered to Montmorillonite, *Clays and Clay Minerals*, V.27, 291-292.
- Kleinsorge, H., 1943, Kızılcahamam sıcak Su Membalarının Tetkiki Hakkında Rapor, MTA Report No: 1415 (Unpublished-Yayımlanmamış).
- Koçyiğit, A., 1991, An Example of An Accretionary Forearc Basin from Northern Central Anatolia and Its Implications For the History of Subduction of Neo-Tethys in Turkey. *Geol.Soc.Am.Bull.*, V.103, 22-36.
- Lumsden, D.N., 1979, Discrepancy Between Thin Sections and X-Ray Estimates of Dolomite in Limestone: *Jour. Sed.Petrology*, V.49, P 429-436.
- Lumsden, D.N. and Chimausky, J.S., 1980, Relationship Between Dolomite Nonstoichiometry and Carbonate Facies Parameters, in D.H. Zenger, J.B.Durham and R.L. Ethington, Eds. *Concepts and Models of Dolomitization: Soc. Econ. Paleontol. Minerals. Spec. Publ. 28*, 123-137.
- Mariner, R.H. and Surdam, R.C., 1970, Alkalinity and Formation of Zeolites in Saline Alkaline Lakes, *Science*, 170, 977-980.
- Mckenzie, J.A., Hsü, K.J. and Schneider, J.F., 1980, Movement of Subsurface Waters Under the Sabkha, Abu Dhabi, UAE, and Its Relation to Evaporative Dolomite Genesis: in D.H. Zenger, J.B.Durham and R.L. Ethington, Eds. *Concepts and Models of Dolomitization: Soc. Econ. Paleontol. Minerals. Spec. Publ. 28*, 11-30.
- Moore, M.D. and Reynolds, R.C., 1989, *X-Ray Diffraction and the Identification and Analysis of Clay Minerals*, Oxford University Press, New York, P.332.
- Morrow, D.W., 1978, the Influence of the Mg/Ca Ratio and Salinity On Dolomitization in Evaporative Basins, *Bull.Canadian. Pet. Geology*, V.26, 389-392.



- Morrow, D.W., 1982, Dolomitization Models and Ancient Dolostones, Geoscience Canada, V.9, 95-107.
- Muir, M.M., Lock, D. and Von Der Borch, C., 1980, the Coroong Model For Penecontemporaneous Dolomite Formation in the Middle Proterozoic Mcarthur Group, Noerthern Territory, Australia, in D.H. Zenger, J.B.Durham and R.L. Ethington, Eds. Concepts and Models of Dolomitization: Soc. Econ. Paleontol. Minerals. Spec. Publ. 28, 51-67.
- Nebert, K., 1959, Anadoludaki Sima Magmatizmasına Ait Silis Teşekkülleri, MTA Bull. V.53, 1-20.
- Nelson C.H., 1967, Sediments of Crater Lake, Oregon, Geol.Soc.Amer.Bull., 78, 833-848.
- Nemecz, E., 1981 Clay Minerals, Akademiai Kiado, Budapest, 547 P.
- Okay, H. and Gürsoy, T., 1984, Kızılcahamam Gerede Jeotermik Enerji Araştırmaları Gravite Etüdü, MTA Report No: 7418, (Unpublished-Yayımlanmamış).
- Olphen, H.V. and Fripat, J.J., 1979, Data Handbook for Clay Minerals and Other Non-Metallic Minerals, William and Sons Ltd., London.
- Öngür, T., 1976, Kızılcahamam, Çamlıdere, Çeltikçi, Kazan Dolayının Jeoliji Durumu ve Jeotermal Enerji Olanakları. MTA Report No: 5669 (Unpublished-Yayımlanmamış).
- Öngür, T., 1977, Kızılcahamam Güneybatısının Volkanolojisi ve Petrolojik İncelemesi, Türkiye Jeoloji Kurumu Bülteni, 20/2, 1-12.
- Özkuzey, S. and Ünsal, Y., 1972, Ankara-Kızılcahamam Perlit Etüdü Hakkında Rapor, MTA Report No: 4763, (Unpublished-Yayımlanmamış).
- Pei-Yuan Chen, 1977, Table of Key Lines in X-Ray Powder Diffraction Patterns of Minerals in Clays and Associated Rocks. USGS Occasional Pap. No: 21, Bloomington, Indiana, 67p.
- Picard, M.D. and High, L.H., 1972, Criteria For Recognising Lacustrine Rocks, in J.K.Rigby and W.M.K.Hamblin, Eds., Recognition of Ancient Sedimentary Environments, Soc. Econ. Paleontol. Minerals. Spec. Publ. 16, 108-145.
- Remy, R.R. and Ferrell, R.E., 1989, Distribution and Origin of Analcime in Marginal Lacustrine Mudstones of the Green River Formation, South Central Uinta Basin, Utah, Clays and Clay Minerals, V.37, 419-432.

- Righi, D., Terribile, F. and Petit, S, 1995, Low-Charge to High-Charge Beidellite Conversion in A Vertisol from South Italy, *Clays and Clay Minerals*, V.43, 495-502.
- Rondot, J., 1956, 1/100.000 lik 39/2 (Güney Kısmı) ve 39/4 Nolu Paftaların Jeolojisi (Seben-Nallıhan-Beypazarı İlçeleri), MTA Report No: 2517 (Unpublished-Yayımlanmamış).
- Schumacher, R. and Schminke, H.U., 1991, Internal Structure and Occurrence of Accretionary Lapilli- A Case Study At Laacher See Volcano, *Bull.Volcanol.*, V.53, 612-634.
- Schumacher, R. and Schminke, H.U., 1995, Models For the Origin of Accretionary Lapilli, *Bull. Volcanol.*, V.56, 626-639.
- Sheppard, R.A., 1989, Zeolitic Alteration of Lacustrine Tuffs, Western Snake River Plain, Idaho, USA, in P.A.Jacobs and R.A. Van Santen (Eds.), *Zeolites: Facts, Figures, Future*, Elsevier, Amsterdam, 501-510.
- Sheppard, R.A., 1991, Zeolitic Diagenesis of Tuffs in the Miocene Chalk Hills Formation, Western Snake River Plain, Idaho, USGS, Bulletin, 1963, P.27.
- Sheppard, R.A., 1994, Zeolitic Diagenesis of Tuffs in Miocene Lacustrine Rocks Near Harney Lake, Harney County, Oregon, USGS Bulletin, 2108, P. 28.
- Sheppard, R.A. and Fitzpatrick, J.J., 1989, Phillipsite from Silicic Tuffs in Saline Alkaline-Lake Deposits, *Clays and Clay Minerals*, V. 37, 243-247.
- Sheppard, R.A. and Gude, A.J., 1968, Distribution and Genesis of Authigenic Silicate Minerals in Tuffs of Pleistocene Lake Tecopa, Inyo County, Calif. U.S. Geol.Surv.Prof.Paper, 597, P.38.
- Smith, G.I, Barczak, V.J., Moulton, G.F. and Liddicoat, 1983, Core Km-3, A Surface-to-Bedrock Record of Cenozoic Sedimentation in Searles Valley, California, USGS, Prof.Pap. 1256, P.24.
- Stamatakis, M.G., 1989 a, A Boron Bearing Potassium Feldspar in Volcanic Ash and Tuffaceous Rocks from Miocene Lake Deposits, Samos Island, Greece., *Amer.Mineral*, 74,230-235.
- Stamatakis, M.G., 1989 b, Authigenic Silicates and Silica Polymorphs in the Miocene Saline-Alkaline Deposits of the Karlovassi Basin, Samos, Greece, *Econ.Geol.*, 84, 788-798.

- Stchepinsky, V., 1942, Beypazarı-Nallıhan-Bolu-Gerede Bölgesi Jeolojisi Hakkında Rapor, MTA Report No: 1363 (Unpublished-Yayımlanmamış).
- Sudo, T., Shimoda, S., Yotsumoto, H. and Aita, S., 1981, Electron Micrographs of Clay Minerals, Developments in Sedimentology 31, Elsevier, Tokyo, P.203.
- Surdam, R.C., 1977, Zeolites in Closed Hydrologic Systems: in Mineralogy and Geology of Natural Zeolites, F.A. Mumpton, Ed., Reviews in Mineralogy, 4, Mineral.Soc.Amer., Washington, D.C., 65-91.
- Surdam, R.C. and Parker, R.D., 1972, Authigenic Aluminosilicate Minerals in the Tuffaceous Rocks of the Green River Formation, Wyoming, Geol.Soc.Amer. Bull., 83, 689-700.
- Surdam, R.C. and Sheppard R.A., 1978, Zeolites in Saline-Alkaline Lake Deposits, in Natural Zeolites: Occurrence, Properties, Use, L.B. Sand and F.A., Mumpton,Eds., Pergamon Press, Elmsford, New York, 145-175.
- Surdam, R.C. and Wolfbauer, C.A., 1975, Green River Formation, Wyoming: A Playa Lake Complex, Geol.Soc.Am.Bull., V 86, 335-345.
- Swain F.M., 1966, Bottom Sediments of Lake Nicaragua and Lake Managua, Western Nicaragua, Jour. of Sed.Petrol. 36, 522-544.
- Şengör, A.M.C. and Yılmaz, Y., 1981, Tethyan Evolution of Turkey: A Plate Tectonic Approach. Tectonophysics, V.75, 181-241.
- Tankut, A., Akıman, O., Türkmenoğlu, A., Güleç, N. and Göker, T., 1990, Tertiary Volkanik Rocks in NW Central Anatolia, Proceedings IESCA 1990 (Int. Earth. Sci. Congr. Aegean Regions). M.Savaşçın and A.H.Eronat (eds.), 2, 450-466.
- Tankut, A., Satır, M., Güleç, N. and Toprak, V., 1995, Galatya Volkaniklerinin Petrojenezi, TUBITAK Report No:YBAG-0059, (Unpublished-Yayımlanmamış).
- Tankut, A. and Türkmenoğlu, A., 1988, Incompatible Trace Element Composition of Neogene Mafic Lavas Around Ankara, METU Jour. Pure and Appl. Sci., 21, 1/3, 501-521.
- Tatlı, S., 1975, Kızılcahamam Doğu Alanının Jeolojisi ve Jeotermal Olanakları, MTA Report No: 5749 (Unpublished-Yayımlanmamış).

- Turgut, T., 1978, Kızılcahamam (Ankara) - Çeltikçi ve Çamlıdere Neojen Havzalarının Linyit Olanakları, MTA Report No: 6173, (Unpublished-Yayımlanmamış).
- Türkecan, A., Hepşen, N., Papak, İ., Akbaş, B., Dinçel, A., Karataş, S., Özgür, İ., Akay, E., Bedi, Y., Sevin, M., Mutlu, G., Sevin, D., Ünay, E. and Saraç, G., 1991, Seben-Gerede (Bolu)-Güdül-Beypazarı (Ankara) ve Çerkeş-Orta-Kurşunlu (Çankırı) Yörelerinin (Köroğlu Dağları) Jeolojisi ve Volkanik Kayaçların Petrolojisi, MTA, Report No: 9193 (Unpublished-Yayımlanmamış).
- Türkmenoğlu, A., Göker, T. and Tankut, A., 1990, Petrography and Mineralogy of Pyroclastic Rocks of the Karaşar District-Beypazarı, Ankara, Proceedings IESCA 1990 (Int. Earth. Sci. Congr. Aegean Regions). M.Savaşçın and A.H.Eronat (Ed), 2, 467-473.
- Ünlü, M.R., 1973, Kazanlar (Bolu) - Peçenek (Ankara) Alanının Jeolojisi ve Jeotermal Olanakları Hakkında Rapor, MTA Report No: 5775 (Unpublished-Yayımlanmamış).
- Van Olphen, H. and Fripat, J.J., 1979, Data Handbook For Clay Minerals and Other Non-Metallic Minerals, Pergamon Press, London, P.346.
- Varol, B. and Kazancı, N., 1980, Seben Bölgesi Volkanotortulları (Bolu GD), Türkiye Jeoloji Kurumu Bülteni, 23/1, 53-58.
- Warren, J.K, 1991, Sulfate Dominated Sea-Marginal and Platform Evaporite Settings: Sabkhas and Salinas, Mudflats and Salterns, in J.L.Melvin, Ed., Petroleum and Mineral Resources, Developments in Sedimentology 50, Elsevier, Amsterdam, P.556.
- Wilson, M.J., 1987, A Handbook of Determinative Methods in Clay Mineralogy. Chapman and Hall, New York, 308 P.
- Wolfbauer, C.A. and Surdam, R.C., 1974, Origin of Non Marine Dolomite in Eocene Lake Gosiute, Green River Basin, Wyoming, Geol. Soc.Amer.Bull., V.85, 1733-1740.
- Yuretich, R.F. and Cerling, E.T., 1983, Hydrochemistry of Lake Turkana, Kenya; Mass Balance and Mineral Reactions in An Alkaline Lake, Geochimica et Cosmochimica Acta, V.47, 1099-1109.
- Yuretich, R.F., Hickey, L.J., Gregson, B.P. and Yuan-Lun Hsia, 1984, Lacustrine Deposits in the Paleocene Fort Union Formation, Northern Bighorn Basin, Montana, Jour.Sed.Petrology, V.54, 836-852.

## **APPENDIX A**

### **PREPARATION OF CLAY SAMPLES FOR X-RAY DIFFRACTION**

#### **1.1. Preparation of Oriented Samples**

##### **1.1.1. General Procedure:**

1. After sieving the sample, 10 grams of sample is placed in a 600 ml. beaker and filled it with deionized water.
2. If necessary, a small quantity of 0.02 M Sodium Pyrophosphate is added to aid dispersion.
3. Sample is put into blender that will be operated for 2 minutes until a good dispersion is achieved.
4. It is necessary to allow the sediment sand sized material to sit long enough. In addition, equivalent settling can be obtained by centrifuging for 2 minutes at 750 rpm.
5. After settling sand-sized material depending on Stoke's law, the suspended material are taken by using a pipette. These particles can be subsided by centrifugation at 600 rpm for 20 min.

6. Smear the resultant material on appropriate sized glass lamellae.

### **1.1.2. Destruction of carbonates:**

1. 10 grams of sample is placed in a beaker and 100 ml. of pH 5 NaOAc buffer is added. Then clay has been brought into suspension by stirring. The suspension is then digested in a near boiling water bath for 30 minutes with occasional stirring.

2. The suspension is centrifuged until the supernatant liquid is clear (Approximately for 10 minutes). Then the liquid is discarded and the remaining precipitate is taken to be stored for other experiments.

3. If the sample is still calcareous additional washing with NaOAc buffer is needed.

### **1.2. Preparation of unoriented samples:**

The clay sample is ground into fine particles and then sieved by using # 200 mesh. After that, a little amount of the sample is packed into an aluminum holder by pressing lightly with a glass slide to obtain a smooth surface which is necessary to get a clear diffraction pattern (Carroll, 1970).

## **APPENDIX B**

### **PREPARATION OF PELLETS FOR INFRARED ANALYSIS**

Sample material after the desired pretreatment is dried at 250°C to remove excess moisture (Jackson, 1975). But in the smectite rich samples 60°C is the temperature used. The sample is (0.1 g of clay) is mixed with 0.9 g of KBr which is dried at 175°C overnight, cooled and ground to pass a 50µm sieve. After the mixture of clay and KBr, the resultant mixture is lightly ground with agate mortar and pestle. The grinding is carried out for sufficiently long time to obtain a homogenous mixture, since random distribution of material yields as precise results. The mixture is pressed in a mold, evacuated and pressed in to a pellet.

## APPENDIX C

### d-SPACING VALUES OF STUDIED K-FELDSPARS, PLAGIOCLASES AND DOLOMITES IN PAZAR FORMATION

	K-feldspars			HKL	Plagioclases		
	2θ CuKa	A	I		2θ CuKa	A	I
**	13.55-13.75	6.53 -6.44	2	110, 110	13.58-13.80	6.52 -6.41	4
				020, 001	(Albite: 13.9)		
				011	18.98-18.9	4.68 -4.69	5-2
	20.95-21.65	4.24 -4.10	10-5	101			
	(Anorthoclase: 21.6-21.9)			201	21.99-22.1	4.04 -4.02	8
M	22.25-22.45	3.99 -3.96	3-1	111			
O	22.54-22.70	3.94 -3.91	2				
M	23.20-23.40	3.83 -3.80	5-2	130			
	23.75-24.05	3.74 -3.70	4-2	130			
O	23.50-23.76	3.78 -3.74	~6	130	23.50-23.76	3.78 -3.74	~6
MP	24.30-24.52	3.66 -3.63	~6	131, 131	24.30-24.52	3.66 -3.63	10-2
	24.51-24.72	3.63 -3.60	~2	131, 131			
	25.05-25.45	3.55 -3.50	1	121, 131			
**	25.5 -25.8	3.49 -3.45	5	112, 112	25.5 -25.7	3.49 -3.46	~5
				221	25.9 -26.15	3.44 -3.41	~3
M-P	26.41-26.71	3.37 -3.33	5	220, 112	26.41-26.5	3.37 -3.36	6-2
	26.8 -27.8	3.34 -3.22	10-6	220			
	(triplet or quadruplet)			201			
	The strongest peak:			040			
	Orthoclase 26.9°			002			
	Sanidine, high 26.8°			002	27.78-28.1	3.21 -3.17	10-8
	Sanidine, low 27.4°			040	(double or triplet)		
	Microcline 27.5°			220			
	Anorthoclase 27.8°			102			
M	29.45-29.65	3.03 -3.01	3-1	131, 131	29.35-29.7	3.04 -3.00	5
O	29.83-30.06	2.99 -2.97	5-	131			
M	30.12-30.24	2.97 -2.96	3	131			
				211, 011	30.3 -30.6	2.95 -2.92	5-2
				131, 132	31.25-31.6	2.86 -2.83	5-2
	30.8	2.90	3-2	022, 041			
	32.3 -32.4	2.77 -2.76	2-1	112			
				132, 134	33.8	2.65	5
	34.7 -34.85	2.58 -2.56	2	221			
				141			
				112			
				241	35.45-35.55	2.53 -2.52	5-2
				211, 112			
	41.6 -41.9	2.17 -2.16	2	060			
				060	42.15-42.6	2.14 -2.12	2
	50.5 -51.1	1.805-1.786	3	104			
	(Anorthoclase: 51.1-51.3)			104	51.2 -51.6	1.783-1.772	3

- \*\* Peak observed in all feldspars.
- \* All plagioclases except albite.
- M Microcline only.
- M-P Peak common in microcline and plagioclase.
- O All K-feldspars except microcline.

Figure C.1.: d spacing and 2 theta values of Feldspars (Pei-Yuan Chen, 1977).



**Table C.1.:  $d$  spacing values of Dolomite**

$d$ (Å)	Intensity
4.033	1
3.699	4
2.888	100
2.670	4
2.539	3
2.404	7
2.193	19
2.065	3
2.015	10
2.006	1
1.8473	3
1.8049	10
1.7870	13
1.7800	2
1.7461	<1
1.5667	2
1.5446	4
1.5403	<1
1.4955	<1
1.4652	2
1.5446	2
1.5403	1
1.4955	1
1.4652	2
1.4435	2
1.4308	1
1.4129	1
1.3885	2
1.3436	<1